

University of Wollongong

## Research Online

---

Faculty of Science, Medicine and Health -  
Papers: part A

Faculty of Science, Medicine and Health

---

1-1-2013

### The emergence of the Eoarchaeon proto-arc: evolution of a c. 3700 Ma convergent plate boundary at Isua, southern West Greenland

Allen Phillip Nutman

*University of Wollongong*, [anutman@uow.edu.au](mailto:anutman@uow.edu.au)

Vickie C. Bennett

*Australian National University*

Clark R L Friend

*Albury View, Tiddington, UK*

Follow this and additional works at: <https://ro.uow.edu.au/smhpapers>



Part of the [Medicine and Health Sciences Commons](#), and the [Social and Behavioral Sciences Commons](#)

---

#### Recommended Citation

Nutman, Allen Phillip; Bennett, Vickie C.; and Friend, Clark R L, "The emergence of the Eoarchaeon proto-arc: evolution of a c. 3700 Ma convergent plate boundary at Isua, southern West Greenland" (2013).

*Faculty of Science, Medicine and Health - Papers: part A*. 1224.

<https://ro.uow.edu.au/smhpapers/1224>

Research Online is the open access institutional repository for the University of Wollongong. For further information contact the UOW Library: [research-pubs@uow.edu.au](mailto:research-pubs@uow.edu.au)

---

# The emergence of the Eoarchaean proto-arc: evolution of a c. 3700 Ma convergent plate boundary at Isua, southern West Greenland

## Abstract

Eoarchaean juvenile crust formed as 'proto-arcs'. The northern side of the Isua supracrustal belt is an archetypal proto-arc, with  $\geq 3720$  Ma boninites, c. 3720 Ma basalts and gabbros, 3720–3710 Ma andesites, diorites and mafic tonalites, 3710–3700 Ma intermediate-felsic volcanic and sedimentary rocks and 3700–3690 Ma chemical sedimentary rocks. On its northern side there is an extensive body of 3700–3690 Ma tonalite. During its evolution, the c. 3700 Ma Isua volcanic–sedimentary assemblage was partitioned into tectonic slices, with intercalation of mantle dunites with pillow basalts, prior to intrusion of c. 3710 Ma quartz diorites. Partitioning also occurred at 3690–3660 Ma, when the 30–20 million years life of the c. 3700 Ma Isua proto-arc was terminated by juxtaposition with the c. 3800 Ma terrane that occurs along the south of the Isua supracrustal belt. The trace element chemistry for all the  $\geq 3720$ –3700 Ma mafic to intermediate volcanic rocks indicates fluid-fluxing mantle melting. The c. 3690 Ma tonalites have signatures showing melting of garnet-bearing mafic (eclogite) sources. The Isua c. 3700 Ma assemblage developed at an intra-oceanic convergent plate boundary, and it has a life-cycle broadly analogous to (but not identical to) an oceanic island arc eventually accreted against older crust.

## Keywords

boundary, plate, ma, isua, southern, 3700, west, c, greenland, evolution, convergent, arc, proto, eoarchaean, emergence, GeoQuest

## Disciplines

Medicine and Health Sciences | Social and Behavioral Sciences

## Publication Details

Nutman, A. P., Bennett, V. C. & Friend, C. R. L. (2014). The emergence of the Eoarchaean proto-arc: evolution of a c. 3700 Ma convergent plate boundary at Isua, southern West Greenland. *Geological Society Special Publication*, 389 (Online first)

1 **Special Publications of the Geological Society, London**  
2 **doi.org/10.1144/SP389.5**

3 **The emergence of the Eoarchaeon proto-arc: evolution of a c. 3700**  
4 **Ma convergent plate boundary at Isua, southern West Greenland**

5  
6 ALLEN P. NUTMAN<sup>1\*</sup>, VICKIE C. BENNETT<sup>2</sup>, CLARK R.L. FRIEND<sup>3</sup>

7  
8 <sup>1</sup> School of Earth & Environmental Sciences, University of Wollongong,  
9 Wollongong,

10 NSW 2522, Australia

11 <sup>2</sup> Research School of Earth Sciences, Australian National University, Canberra,  
12 ACT 0200, Australia

13 <sup>3</sup> Gendale, Albury View, Tiddington, Oxon, OX9 2LQ, UK

14

15

16 \* Corresponding author: Allen Nutman (*e-mail:anutman@uow.edu.au*)

17

18

19 **Abstract:** Eoarchaean juvenile crust formed as ‘proto-arcs’. The northern side of the Isua  
20 supracrustal belt is an archetypal proto-arc, with  $\geq 3720$  Ma boninites, *c.* 3720 Ma basalts and  
21 gabbros, 3720-3710 Ma andesites, diorites and mafic tonalites, 3710-3700 Ma  
22 intermediate-felsic volcanic and sedimentary rocks and 3700-3690 Ma chemical sedimentary  
23 rocks. On its northern side there is an extensive body of 3700-3690 Ma tonalite. During its  
24 evolution the *c.* 3700 Ma Isua volcanic-sedimentary assemblage was partitioned into tectonic  
25 slices, with the intercalation of mantle dunites with pillow basalts, prior to intrusion of *c.* 3710  
26 Ma quartz diorites. Partitioning also occurred at 3690-3660 Ma, when the 30-20 million years  
27 life of the *c.* 3700 Ma Isua proto-arc was terminated by juxtaposition with the *c.* 3800 Ma  
28 terrane that occurs along the south of the Isua supracrustal belt. The trace element chemistry for  
29 all the  $\geq 3720$ -3700 Ma mafic to intermediate volcanic rocks indicates fluid-fluxing mantle  
30 melting. The *c.* 3690 Ma tonalites have signatures showing melting of garnet-bearing mafic  
31 (eclogite) sources. The Isua *c.* 3700 Ma assemblage developed at an intra-oceanic convergent  
32 plate boundary, and that it has a life cycle broadly analogous (but not identical to) an oceanic  
33 island arc eventually accreted against older crust.

34 **Keywords:** Eoarchaean proto-arc, Juvenile crust, Island arcs, Convergent plate boundaries,  
35 Weathering  
36

37 Strontium, Nd and Hf radiogenic isotope data from the rare surviving oldest rocks  
38 (4000-3600 Ma; approximately a millionth of the present crust) indicate that they  
39 represent largely juvenile Eoarchaeon crust (Moorbath, 1975; Hamilton *et al.*, 1978;  
40 Baadsgaard *et al.*, 1986a; Collerson *et al.*, 1991; Bennett *et al.*, 1993, 2007; Caro *et al.*,  
41 2005; Hiess *et al.*, 2009). One school of thought proposes that surviving Eoarchaeon  
42 crust, exemplified by that found in the Itsaq Gneiss Complex of Greenland, formed at  
43 convergent plate boundaries due to fluid-fluxing of mantle and/or melting of  
44 subducted mafic crust, i.e. in an environment akin to modern island arcs (e.g., Nutman  
45 *et al.*, 1999, 2007; Polat *et al.*, 2002; Polat & Hoffman, 2003; Jenner *et al.*, 2009;  
46 Nagel *et al.*, 2012). Alternatively, based solely on the Hf isotopic signatures of zircons  
47 from ancient orthogneisses, a non-plate tectonic mechanism of Eoarchaeon crust  
48 formation was proposed by Næraa *et al.* (2012). Other tectonic settings for crust  
49 formation have been provided by Shirey & Richardson (2011) and Dhuime *et al.*  
50 (2012).

51         However, other lines of evidence besides radiogenic isotopic signatures are  
52 important in elucidating the origin and evolution of crust. This is because these  
53 signatures only indicate whether newly-formed crust is juvenile or involves melting of  
54 older continent-like crust, and reveals nothing concerning the *melting mechanism* and  
55 *tectonic setting* of crust formation. Thus structural geology data (e.g., Nutman, 1984,  
56 Nutman *et al.*, 2002; Komiya *et al.*, 1999), whole rock geochemistry signatures (e.g.,  
57 Nutman *et al.*, 1999; Polat & Hofmann, 2003; Hoffmann *et al.*, 2011a) and accurate  
58 and precise absolute dates (particularly by U-Pb zircon methods) should be integrated  
59 with the isotopic data (e.g., Bennett *et al.*, 2007; Hoffmann *et al.*, 2011b).  
60 Consequently, a multidisciplinary data set offers the best constraints on the  
61 geodynamic setting of crust formation and provides insight into the meaning of  
62 changing palaeogeographic settings (such as marine transgressions and regressions). In  
63 this paper we follow this holistic approach, and apply it to the *c.* 3700 Ma portion of  
64 the Isua supracrustal belt (West Greenland; Fig. 1), which is the world's best preserved  
65 example of Eoarchaeon crust formation. For the Isua supracrustal belt we conclude that  
66 scenarios analogous with, but not identical to, island-arc settings best fit the  
67 multidisciplinary data. We introduce here the term *proto-arc* for these ancient rock  
68 assemblages. We then explore how in detail the architecture of proto-arcs might have  
69 differed from that of Phanerozoic arcs.

70

71 **The oldest geological record and the Isua supracrustal belt**72 *The Eoarchaean geological record*

73 The rare occurrences of 4000-3600 Ma (Eoarchaean) rocks reflect the small  
74 volume of them that have survived more than 3.5 billion years of plate tectonics,  
75 weathering and erosion (Nutman, 2006 and references therein). Such old rocks occur  
76 as variably preserved remnants in several gneiss complexes around the world (the Itsaq  
77 Gneiss Complex of Greenland, Uivak Gneisses of Labrador, Narryer Gneiss Complex  
78 of Western Australia, Acasta Gneisses of the Northwestern Territories and gneisses in  
79 the Anshan area of northeastern China; for summaries of these see Schiøtte *et al.*,  
80 1989; Nutman *et al.*, 1991, 1996; Kinny & Nutman, 1996; Bowring & Williams, 1999;  
81 Iizuka *et al.*, 2007; Liu *et al.*, 2007; O'Neil *et al.*, 2007 and Horie *et al.*, 2010). The  
82 ~3000 km<sup>2</sup> Itsaq Gneiss Complex of the Nuuk district of southern West Greenland is  
83 the best exposed with some areas of relatively low strain and low metamorphic grade  
84 (Nutman *et al.* 1996 and references therein). These attributes mean that data from  
85 the Itsaq Gneiss Complex are important in of studies towards a better understanding of  
86 the Eoarchaean Earth.

87

88 *Itsaq Gneiss Complex*

89 Much of the Itsaq Gneiss Complex was affected by 3660-3600 Ma high-grade  
90 metamorphism and ductile deformation (Griffin *et al.*, 1980, Nutman *et al.*, 1996;  
91 Friend & Nutman 2005a), such that by *c.* 3600 Ma its lithologies had been widely  
92 converted into strongly deformed, multi-component, amphibolite-granulite facies  
93 gneisses (McGregor, 1973; Nutman *et al.*, 2000). An additional complication in  
94 interpreting the Itsaq Gneiss Complex is that it occurs as tectonic slivers bounded by  
95 folded Meso- and Neoproterozoic meta-mylonites, within a collage of younger Archaean  
96 terranes that were assembled into their present configuration by the end of the  
97 Archaean (Friend *et al.*, 1987, 1988; Nutman *et al.*, 1989, Nutman & Friend, 2007;  
98 Crowley, 2002; Friend & Nutman, 2005b).

99 The later Archaean tectonothermal overprints mean that at most localities it is  
100 hard to extract any detailed information concerning the early history of the Itsaq Gneiss  
101 Complex. Fortunately, around the *Isua supracrustal belt* at the Itsaq Gneiss Complex's  
102 northern extremity (Fig. 1), there are domains that are least affected by later Archaean

103 tectonothermal overprinting which provide a window onto the early Earth's crust. This  
104 allows (a) study of the earliest tectonic evolution (e.g. Nutman, 1984; Nutman *et al.*,  
105 1984, 2002, Komiya *et al.*, 1999; Nutman & Friend, 2009), (b) provides the most  
106 robust geochemical and isotopic interpretations because individual Eoarchaeon crustal  
107 components can be sampled separately (e.g., Baadsgaard *et al.*, 1986a; Nutman *et al.*,  
108 1996, 1999; Friend *et al.*, 2002; Crowley *et al.*, 2002; Polat *et al.*, 2002; Polat &  
109 Hofmann, 2003; Bennett *et al.*, 1993, 2003, 2007; Hiess *et al.*, 2009), (c) gives insight  
110 into volcanic and sedimentary environments, (d) perhaps containing evidence of the  
111 earliest life habitats (Schidlowski *et al.*, 1979; Rosing, 1999; Dauphas *et al.*, 2004;  
112 Nutman *et al.*, 2010; Craddock & Dauphas, 2011) and (e) allows understanding of  
113 Earth's early climate (Rosing *et al.*, 2010; Nutman *et al.*, 2012a).

114

#### 115 *The Isua supracrustal belt*

116         Within the Itsaq Gneiss Complex the most important unit of supracrustal rocks  
117 is the Isua supracrustal belt. The belt is c. 35 km long by up to 2.5 km wide (Fig. 1). To  
118 the east it is covered by the edge of the Inland Ice. To the north and south, the belt is  
119 bounded by metaplutonic complexes, with that on the north dominated by 3700-3690  
120 Ma tonalite protoliths with c. 3650 Ma granite sheets, and that to the south dominated  
121 by 3820-3795 Ma tonalite protoliths (Nutman *et al.*, 1996, 1997, 2000; Crowley *et al.*,  
122 2002; Crowley, 2003; Nutman & Friend, 2009). In southern part of the belt, intrusive  
123 tonalite sheets are more common than in the north, and intrude already deformed  
124 metabasaltic rocks. To the west the belt is in tectonic contact with Mesoarchaeon  
125 gneisses and supracrustal rocks (Nutman & Friend, 2009).

126         Despite that the Isua supracrustal belt largely escaped Neoarchaeon  
127 deformation, most of the belt was already strongly deformed in the Eoarchaeon. This  
128 means that outcrop-scale compositional layering is mostly of transposed tectonic  
129 origin (Nutman *et al.*, 1984, 1996, 2002, 2007; Myers, 2001). Thus, it is only in a few  
130 places that primary volcanic and sedimentary structures have survived (e.g., Nutman *et*  
131 *al.*, 1984; 1997, 2007; Komiya *et al.*, 1999; Solvang, 1999; Furnes *et al.*, 2007).

132 Plutonic rocks are much less common within the belt, but include some gabbros and  
133 ultramafic rocks that were derived from both layered gabbro intrusion cumulates and  
134 from the mantle (e.g., Dymek *et al.*, 1988; Friend & Nutman, 2011).

135         Initial age constraints of the Isua supracrustal belt rocks were Rb-Sr whole rock  
136 Eoarchaeon errorchrons (linear scatters of data which give an approximate ages with

137 errors of >100 million years) for orthogneiss components invading and proximal to the  
138 belt (Moorbath *et al.*, 1972, 1977), a whole rock Pb-Pb  $3710 \pm 70$  Ma errorchron on a  
139 banded iron formation unit (Moorbath *et al.*, 1973), and a Sm-Nd  $3770 \pm 42$  Ma  
140 errorchron for a mixed suite of felsic and mafic rocks (Hamilton *et al.*, 1978). Within  
141 this early geochronological framework, it was considered that the Isua supracrustal  
142 rocks were all related, albeit partitioned by early tectonic breaks (Nutman *et al.*, 1984).  
143 Subsequently, with uncertainties of  $\leq \pm 10$  Ma, SHRIMP U-Pb zircon dating  
144 demonstrated that the belt contained supracrustal rocks varying in age by 100 million  
145 years. Hence the belt's southern part is dominated by *c.* 3800 Ma rocks, whereas along  
146 its northern and central portions there are *c.* 3700 Ma rocks (Fig. 1; Nutman *et al.*,  
147 1996, 1997). Nutman *et al.* (1997) proposed that these unrelated sequences were  
148 separated by Eoarchaean mylonites, and this basic principle has stood independent  
149 tests of integrated detailed field work with zircon U-Pb geochronology by Crowley  
150 (2003) and Kamber *et al.* (2005) and has been expanded upon in more recent work  
151 (Nutman & Friend, 2009; Nutman *et al.*, 2002, 2009; Friend & Nutman, 2010). The  
152 younger, *c.* 3700 Ma supracrustal and plutonic rocks along the northern side of the Isua  
153 supracrustal belt overall have the most areas of low rare low strain of all the Itsaq  
154 Gneiss Complex is therefore the most amenable one to provide information on the  
155 origin and evolution of Eoarchaean crust.

156

### 157 **Detailed evolution of the *c.* 3700 Ma portion of the Isua supracrustal belt**

#### 158 *Lithologies and U-Pb zircon geochronology*

159 The *c.* 3700 Ma portion of the Isua supracrustal belt comprises tectonically  
160 imbricated slices of mostly strongly deformed, amphibolitised pillow lavas and lesser  
161 amounts of gabbro and cumulate ultramafic rocks, felsic schists with andesite-dacite  
162 protoliths, metasedimentary mica-rich schists derived from volcanic sources, chemical  
163 sedimentary rocks and depleted mantle dunite (e.g., Allaart, 1976; Nutman *et al.*, 1984,  
164 2009, Polat *et al.*, 2002; Polat & Hofmann, 2003; Bohlar *et al.*, 2004, 2005; Kamber *et al.*  
165 *et al.*, 2005; Friend *et al.*, 2007; Friend & Nutman, 2011).

166 The amphibolites have two main variants, a high Mg/Fe one that in early  
167 studies was known as the *garbenschiefer unit* (e.g., Allaart *et al.*, 1976, Gill *et al.*,  
168 1981; Nutman *et al.*, 1984) and the other is a lower Mg/Fe type. These form mutually  
169 exclusive mappable units (Nutman *et al.*, 1984, 2002; Nutman & Friend, 2009). The  
170 high Mg/Fe variety (*garbenschiefer*) has boninitic affinities, whereas the lower Mg/Fe



171 varieties are geochemically akin to arc basalts (showing features such as enrichment of  
172 the light rare earth elements and Nb and Ti depletions; Polat *et al.*, 2002; Polat &  
173 Hoffman, 2003; see below). Both varieties are dominated by volcanic protoliths, with  
174 sporadic but overall rare preservation of pillow structure (e.g., Komiya *et al.*, 1999;  
175 Furnes *et al.*, 2007, 2009; Friend & Nutman, 2010). In a rare low strain area in the west  
176 of the belt (Fig. 2), layered gabbro with amphibolitised relict igneous texture occurs  
177 within boninitic pillow lavas and contains high Th/U igneous zircons with an age of  
178  $3717 \pm 11$  Ma (Nutman & Friend, 2009). Boninitic amphibolites with relict pillow  
179 structure are also cut by a  $3712 \pm 6$  Ma hypabyssal mafic tonalite sheet (Nutman &  
180 Friend, 2009). These precise U-Pb zircon minimum ages indicate that the boninitic  
181 amphibolites are  $\geq 3720$ - $3710$  Ma old, in accord with less precise whole rock Sm-Nd  
182 and Lu-Hf age determinations on them of  $3756 \pm 200$  Ma to  $3825 \pm 160$  Ma (Hamilton  
183 *et al.*, 1978; Hoffmann *et al.*, 2010). The  $3717 \pm 11$  Ma leucogabbro sheet that cuts  
184 boninitic metabasalts has arc-basalt chemical affinities (sample G07/26 – below), and  
185 might give an absolute age determination on the regional lower Mg/Fe basalts. In the  
186 northern end of the belt,  $3717 \pm 6$  Ma diorites (Friend & Nutman, 2010) intrude lower  
187 Mg/Fe amphibolites.

188         Ultramafic rocks occur as lenses within the *c.* 3700 Ma amphibolite sequences.  
189 Most of these are highly altered and modified, and now occur as variably carbonated  
190 amphibole, serpentine and locally talc-bearing schists. Some of these represent  
191 dismembered, altered cumulate portions of gabbro intrusions (Dymek *et al.*, 1988), but  
192 one strand of ultramafic schists in the western end of the belt (Figs. 2 and 3) contains  
193 two large pods (*c.* 50 x 100 m and 100 x 500 m) of variably-altered but locally fresh  
194 dunite, which have depleted mantle chemical signatures, such as depletion of the light  
195 rare earth elements, extremely low Al, Ca and Ti contents and being dominated by *c.*  
196 Fo<sub>90</sub> olivine (Friend & Nutman, 2011).

197         Layered felsic mica schists are most extensive in the eastern end of the belt  
198 (Fig. 1). They locally preserve agglomerate structures and graded layering (Nutman *et*  
199 *al.*, 1984, 1997) and are thus most likely of volcanic or volcano-sedimentary origin.  
200 These rocks contain 3710-3700 Ma igneous zircons, showing they are marginally  
201 younger than intercalated mafic volcanic rocks (Nutman *et al.*, 2009). Mafic  
202 mica-garnet rich schists are found interspersed with the felsic schists, and are derived  
203 from weathered mafic igneous sources (Nutman *et al.*, 1984, 2012a; Bohlar *et al.*,  
204 2005). The mafic schists have given sparse yields of small prismatic zircons with

205 3710-3700 Ma ages (Kamber *et al.*, 2005) – confirming that they are coeval with the  
206 associated felsic mica schists.

207 Major units of non-detrital sedimentary rocks occur with the *c.* 3700 Ma  
208 volcanic rocks (Moorbath *et al.*, 1973; Allaart, 1976). These yield sparse, small  
209 (typically *c.* 50  $\mu\text{m}$  long), euhedral, oscillatory-zoned zircons, with ages of 3695-3690  
210 Ma (Nutman *et al.*, 2002, 2009). These are interpreted as small amounts of  
211 volcanogenic material incorporated into the chemical sedimentary rocks, possibly as  
212 ash, and thereby give a proxy for their true age (Nutman *et al.*, 2002, 2009). These  
213 chemical sedimentary rocks vary from chert, to layered quartz + magnetite banded iron  
214 formation, to calc-silicate rocks and dolomitic marbles. The cherts and banded iron  
215 formations have always been accepted as having sedimentary protoliths (onwards from  
216 Moorbath *et al.*, 1973 and Allaart, 1976). However the protoliths for the calc-silicate  
217 rocks and marbles have been disputed. Some authors suppose that they are entirely  
218 metasomatic in origin (e.g. Rosing *et al.*, 1996), contesting earlier interpretations that  
219 at least some have sedimentary/surficial protoliths (Allaart, 1976; Nutman *et al.*,  
220 1984). The sedimentary interpretation is supported by modern detailed geochemical  
221 and stable isotope studies because at least some of them display a seawater-like  
222 REE+Y (rare earth element + yttrium) trace element signature (Friend *et al.*, 2007),  
223 and because they display Fe isotopic fractionation indicative of biomediation  
224 (Craddock & Dauphas, 2011). Thus although it is widely acknowledged that the belt  
225 has been subjected to metasomatism with carbonate veining, there is increasing  
226 evidence that at least some of the carbonates are of sedimentary/surficial origin. It also  
227 now appears that biomediation probably played a part in their development (Craddock  
228 & Dauphas, 2011; Nutman *et al.*, 2010).

229  $\geq 3700$  Ma supracrustal rocks of the Isua supracrustal belt, locally intruded by  
230 3720-3710 Ma quartz diorites and mafic tonalites, are in early tectonic contact with a  
231 northern domain of 3700-3690 Ma tonalitic gneisses intruded by *c.* 3650 Ma granite  
232 sheets (Fig. 1; Nutman *et al.*, 1996, 2000, 2002; Crowley *et al.*, 2002). This 3700-3690  
233 Ma tonalite domain, or a volcanic carapace eroded off it, could be representative of the  
234 distal source for the rare, small oscillatory-zoned zircons in the chemical sedimentary  
235 rocks of the *c.* 3700 Ma part of the belt.

236

237 *Submarine and subaerial environments*

238 In low strain zones scattered throughout the belt,  $\geq 3720$  Ma both boninitic and  
239 lower Mg/Fe amphibolites locally preserve pillow structures. In a low strain zone in  
240 the east of the belt (Fig. 4, locality A), more evolved mafic-intermediate volcanic rocks  
241 also preserve pillow structures (Solvang, 1999), and these have yielded a single  
242 oscillatory-zoned prismatic zircon with an age of  $3709 \pm 9$  Ma (Nutman *et al.*, 2010).  
243 This indicates that submarine conditions continued until at least *c.* 3710 Ma.

244 Based on the facing direction of the relict pillow structures in low strain zone A  
245 on Fig. 4, the *c.* 3710 Ma mafic-intermediate pillowed rocks are stratigraphically the  
246 lowest, and face up to a unit of chemical sedimentary rocks. Sparse 3695-3690 Ma  
247 volcanogenic zircons within the chemical sedimentary rocks are taken as giving their  
248 time of deposition (Fig. 4; Nutman *et al.*, 2002, 2009). The structural and stratigraphic  
249 top of the chemical sedimentary rocks is terminated by a mylonite, above which there  
250 is an allochthonous body of  $\geq 3720$  Ma boninitic amphibolites. The boundary between  
251 the underlying pillowed mafic-intermediate volcanic rocks and the chemical  
252 sedimentary rocks is not a tectonic break (albeit it is deformed). Our preferred  
253 interpretation, supported by geochemical evidence given below, is that the underlying  
254 pillowed submarine volcanic rocks were uplifted, subaerially exposed, weathered and  
255 eroded, prior to a transgression and deposition of the chemical sedimentary rocks on  
256 top of them at 3695-3690 Ma.

257 The accrued geological, geochronological and geochemical data are evidence  
258 for contrasting volcanic and sedimentary environments, from (deep) marine for the  
259 early basalts to at least locally subaerial between 3710 and 3695 Ma and then  
260 submarine again for the 3695-3690 Ma chemical sedimentary rocks.

261

#### 262 *Whole rock geochemistry of igneous rocks*

263 Polat *et al.*, (2002) and Polat & Hofmann (2003) showed that with careful  
264 sampling, Isua mafic igneous rocks with close to original igneous geochemical  
265 composition can be selected. This is borne out in the mafic igneous (M), felsic igneous  
266 (F) and weathering (W) ternary plot of Ohata & Arai (2007; Fig. 5; see figure caption  
267 for more information on this plot), where 'fresh' well-preserved metabasaltic rocks of  
268 both categories plus leucocratic metagabbros of the lower Mg/Fe suite coincide with  
269 the igneous trend in this diagram (Table 1, Fig. 5). The centres of well-preserved  
270 pillows in basalts of lower Mg/Fe island arc affinity show  $\delta^{18}\text{O}$  values of +9.9 to +6.3  
271 (Furnes *et al.*, 2007), typical of those found in younger submarine settings, with the

272 variation considered to reflect hydrothermal effects immediately following eruption.  
273 Likewise, well-preserved (i.e. with relict igneous texture) more evolved igneous rocks  
274 fall exactly on the igneous trend M-F igneous trend on the M-F-W plot; 3720-3710 Ma  
275 diorites and mafic tonalites (samples 229404, G07/25 and G07/28) and the c. 3690 Ma  
276 tonalites (such as sample G07/41; Table 1, Fig.5). Indication of the freshness of these  
277 rocks is given by 'mantle-like' whole rock  $\delta^{18}\text{O}$  values between +7 to +8 for samples  
278 229404 and 225893 (Baadsgaard *et al.*, 1986b).

279         Alteration of the igneous chemistry of the c. 3700 Ma igneous rocks could have  
280 been by metasomatism or Eoarchaeon weathering. Superimposed metasomatism can  
281 be due to focused-flow fluid-dominant regimes during later tectonothermal events (e.g.  
282 Nutman *et al.*, 1984; Rosing *et al.*, 1996). Field evidence such as coarse-grained quartz  
283 or carbonate veining and growth of coarse mica can discriminate such cases, and such  
284 rocks have been avoided in sampling (e.g., Polat & Hofmann, 2003; Jenner *et al.*,  
285 2009; Hoffmann *et al.*, 2010). Strong ductile deformation with distributed fluid flow  
286 may also provide an opportunity for marked modification in the chemistry of the rocks.  
287 This can be assessed by comparing the chemistry of Isua metavolcanic rocks from low  
288 and high ductile strain domains. In the rare low strain domains pillow structures are  
289 preserved, but generally Eoarchaeon (i.e., prior to the intrusion of the ~3500 Ma  
290 Ameralik dykes) ductile high strain converted the 'boninitic' rocks into magnesian  
291 chlorite + orthoamphibole + plagioclase schists, whereas the lower Mg/Fe basalts were  
292 converted into strongly layered hornblende + plagioclase amphibolites. On an MFW  
293 plot, the compositions of the strongly deformed rocks from both categories are  
294 congruent with their less deformed counterparts (Fig. 5 and its legend). This  
295 demonstrates that the superimposed ductile deformation did not modify the major  
296 element chemistry of the rocks to the extent it could be detectable on such plots.  
297 Immobility is also apparent for elements such as the REE and HFSE that are used to  
298 discriminate different petrogenesis of igneous suites. This is shown by comparing the  
299 trace element pattern for low strain pillowed amphibolites such as G05/32, -33 with  
300 highly strained, flaggy amphibolite G93/18 from the same unit (Fig. 6a).

301         A second scenario to modify whole rock chemistry is weathering, particularly  
302 in a subaerial setting. At localities A and B (Fig. 4) the major element chemistry of the  
303 c. 3710 Ma volcanic rocks unconformably overlain by chemical sedimentary rocks of  
304 deviates from igneous trends in the MFW plot, with a strong dispersion from the M-F  
305 trend towards W. Such deviations from undisturbed geochemical trends are focused

306 stratigraphically underneath a younger, overlying chemical sedimentary unit.  
307 Furthermore, 3710-3700 Ma volcano-sedimentary rocks that are low strain and lacking  
308 in evidence of metasomatism via veining show variable but mostly considerable  
309 deviation towards W off the M-F igneous trend. This suggests that prior to or during  
310 deposition, material forming them had been subjected to variable degrees of subaerial  
311 weathering (Nutman *et al.*, 2012a; Fig. 5).

312 Our selection of mafic whole rock geochemical data (Table 2) replicates the  
313 results of the more extensive studies of Polat *et al.* (2002) and Polat & Hofmann  
314 (2003), with enrichment of the LREE over the HREE and negative Nb, Ta and Ti  
315 anomalies (Fig. 6A). Using combinations of elements considered as immobile (at least  
316 in rock-dominated tectonic systems), location of the data in the volcanic arc field in  
317 plots such as Nb/Yb versus Th/Yb (Fig. 6B) indicate the importance of fluid-fluxing of  
318 upper mantle sources in forming the boninites and the lower Mg/Fe basalts that are of  
319 arc affinity (see Eggins, 1993 for explanation of the fluid fluxing mechanism  
320 geochemical signatures). Rare gabbro bodies (such as G07/26 with a U-Pb zircon age  
321 of  $3717 \pm 11$  Ma that occurs with boninitic amphibolites) also have arc-basalt affinity  
322 (Fig. 6). The same applies for somewhat more evolved volcanic rocks such as the  
323 slightly younger ( $3709 \pm 9$  Ma) varieties around locality A in Fig. 4 – which have a  
324 more andesitic affinity (Table 1, Fig. 6).

325 On the SiO<sub>2</sub> versus MgO plot the older (3720-3710 Ma) plutonic rocks are  
326 mostly low SiO<sub>2</sub> and high MgO (Fig. 7A). These can be broadly classified as  
327 quartz-diorites, apart from G07/25 that is a high-Mg tonalite. On discriminant  
328 diagrams such as Y versus Sr/Y and Yb<sub>(N)</sub> versus La/Yb<sub>(N)</sub> the lower silica 3720-3710  
329 Ma plutonic rocks fall in the field of typical arc rocks (Fig. 7B,C). Most likely their  
330 origin was dominated by melts produced by fluid fluxing of mantle (see Martin *et al.*,  
331 2005). It should be noted also that these rocks have trace element patterns and Nb/Yb  
332 and Th/Yb very similar to c. 3710 Ma andesites (such as samples at locality A, Fig. 4;  
333 see the data for plutonic rocks G07/28 and G05/25 placed onto Fig. 6). This indicates  
334 that they are simply plutonic and volcanic manifestations of the same igneous event.

335 The 3700-3690 Ma tonalites that form the large allochthonous mass north of  
336 the belt are geochemically distinct, with higher SiO<sub>2</sub> and much lower MgO (Fig. 7A).  
337 In Y versus Sr/Y and Yb<sub>(N)</sub> versus La/Yb<sub>(N)</sub> discriminant plots (Figs. 7B,C), some of  
338 the samples fall in the field of typical adakites whereas others lie in the region where  
339 adakites and typical arc compositions overlap. Based on this alone, the younger suite

340 could have formed by melting of mafic rocks under high pressure (eclogite or garnet  
341 amphibolite; c.f., Martin, 1986; Martin *et al.*, 2005) or by (extensive) fractional  
342 crystallisation of more mafic arc magmas (MacPherson *et al.*, 2006). However there is  
343 a major volume problem with the latter model, because the  
344 tonalite-trondhjemite-granodiorite suites form approximately 90% of the Eoarchean  
345 crust. It is now documented that early tectonic intercalation has juxtaposed upper  
346 mantle and upper crustal rocks (Nutman *et al.*, 1996; Friend *et al.*, 2010). Why then is  
347 there not ample evidence of *lower crustal* cumulates complementing the  
348 tonalite-trondhjemite-granodiorite suites in the Eoarchean geological record? This  
349 volume problem is resolved if the tonalite-trondhjemite-granodiorite suites formed by  
350 partial melting of mafic rocks buried by underthrusting into the stability field of  
351 eclogite. In which case, the complementary very dense resitites reside in the mantle.

352

353 *≥3650 Ma tectonism*

354 Mapping combined with U-Pb zircon geochronology shows that within the *c.*  
355 3700 Ma part of Isua, rocks were tectonically intercalated prior to intrusion of the *c.*  
356 3510 Ma Ameralik (metabasic) dykes (Nutman *et al.*, 1984, 2007, 2009; Komiya *et al.*,  
357 1999; Nutman & Friend, 2009). There are several episodes of tectonic intercalation.  
358 Thus at the eastern margin of northwestern portion of the belt (Fig. 2), *c.* 3720 Ma low  
359 Mg/Fe amphibolites of island arc basalt affinity with rare relicts of pillow structure  
360 (e.g., Furnes *et al.*, 2007) are tectonically intercalated with upper mantle dunites  
361 (Friend & Nutman, 2011). This tectonic intercalation is older than the intrusion of the  
362  $3717 \pm 6$  Ma diorites to the east (Friend & Nutman, 2010). Within the northwestern  
363 part of the belt, *c.* 3690 Ma banded iron formation is tectonically intercalated with  
364 felsic schists bearing 3724-3712 Ma volcanic or sedimentary zircons (G05/28+29 in  
365 Fig. 2). In turn, these intercalated rocks occur as a tectonic sliver within  $\geq 3717$  Ma  
366 boninitic amphibolites. In the eastern part of the belt, a tectonic (folded thrust) contact  
367 between *c.* 3690 Ma metachert with banded iron formation and tectonically overlying  
368 boninitic amphibolite has been intruded by a gabbro sheet (Fig. 4). Along strike to the  
369 southwest, where this sheet lies entirely within pillowed boninitic amphibolites, it has  
370 yielded sparse high Th/U  $3643 \pm 6$  Ma zircons, interpreted as giving the magmatic age  
371 (sample G97/87 in Nutman *et al.*, 2002). This indicates that the thrusting of the  
372 boninitic rocks over *c.* 3690 Ma chemical sedimentary rocks occurred before 3643 Ma.

373           There are also younger Eoarchaean shear zones and tectonic breaks in the Isua  
374 supracrustal belt. The most important of these is the tectonic break separating the *c.*  
375 3800 Ma rocks in the south of Isua from the *c.* 3700 Ma rocks to the north (Fig. 1). This  
376 break has been interpreted as a tectonically reactivated suture, marking the  
377 juxtaposition of *c.* 3800 and *c.* 3700 Ma terranes. This occurred between *c.* 3690 Ma  
378 (youngest rocks unique to the northern terrane) and 3660 Ma, the age of the first rocks  
379 common to both terranes (Crowley, 2003; Nutman & Friend, 2009). North of, and  
380 sub-parallel to this important boundary, there are other mylonites. These mylonites  
381 partition the *c.* 3700 Ma assemblage into sub-terranes, and thereby also truncate earlier  
382 tectonic breaks described above (Nutman & Friend, 2009). These are commonly  
383 marked by synkinematic pegmatites with flaser structure that yield ages of 3650-3640  
384 Ma (Crowley *et al.*, 2002; Nutman *et al.*, 2002). These breaks are regarded as relating  
385 to extensional partitioning of crust that had been thickened a short time before during  
386 the juxtaposition of the 3800 Ma and 3700 Ma terranes (Nutman *et al.*, 2012b).

387

## 388 **Discussion**

### 389 *Juvenile crust*

390           All samples from the *c.* 3700 Ma supracrustal assemblage and the tonalite  
391 domain to the north have whole rock initial  $\epsilon_{Nd}$  values of  $\geq +1$  and near-chondritic  
392 zircon and whole rock initial  $\epsilon_{Hf}$  values of *c.*  $0 \pm 1$  (Hamilton *et al.*, 1978; Jacobsen &  
393 Dymek, 1987; Baadsgaard *et al.*, 1986a; Moorbath, 2005; Polat *et al.*, 2002; Hiess *et*  
394 *al.*, 2009; Rizo *et al.*, 2011; Hoffmann *et al.*, 2011b, Rizo *et al.*, 2011, Næraa *et al.*,  
395 2012). The single exception is the  $\geq 3720$  Ma boninitic metabasalts, with initial  $\epsilon_{Hf}$   
396 values of up to + 12 (Hoffmann *et al.*, 2010). Furthermore, all zircons within  
397 sedimentary rocks of the *c.* 3700 Ma terrane are 3740-3690 million years old, in stark  
398 contrast to the *c.* 3800 Ma terrane to the south where detrital grains up to 3940 million  
399 years old have been recorded in sedimentary rocks (Nutman *et al.*, 2009). This shows  
400 that the *c.* 3700 Ma assemblage is essentially juvenile – with no detectable input from  
401 older (3940-3800 Ma) sialic crust exposed immediately south of the suture running  
402 through the Isua supracrustal belt (Fig. 1).

403           Geochemical evidence such as depletion of Nb and Ta (Fig. 6) indicates that mafic to  
404 intermediate igneous rocks in the *c.* 3700 Ma terrane involved fluid-fluxing of upper  
405 mantle sources (Polat *et al.*, 2002; Polat & Hofmann, 2003). Igneous rocks represented

406 by the extensive 3700-3690 Ma tonalite outcrops north of the Isua supracrustal belt  
407 have geochemical signatures (e.g. high La/Yb<sub>(N)</sub> and low Yb<sub>(N)</sub>) that according to  
408 widely accepted interpretations (Martin, 1986; Martin *et al.*, 2005; Hoffmann *et al.*,  
409 2011a) are indicative of melting eclogites and/or high pressure granulites. Combined  
410 with the U-Pb zircon geochronology (Nutman & Friend, 2009) this shows a temporal  
411 progression of melting mechanisms from early mantle fluid-fluxing ( $\leq 3720$ -3710 Ma)  
412 to melting high pressure mafic rock sources (3700-3690 Ma).

413

#### 414 *Tectonically active environment*

415 Development of the igneous assemblages took place in a tectonically active  
416 environment, such that by 3717 Ma, metabasalts had been tectonically intercalated  
417 with slices of upper mantle dunite (Fig. 2; Friend & Nutman, 2010, 2011), and by 3643  
418 Ma andesites and basalts capped by 3690 Ma chemical sedimentary rock had  $\geq 3720$   
419 Ma boninites thrust over them (Localities A and B in Fig. 4). Further evidence for the  
420 tectonically active environment comes from the variable degree of *c.* 3700 Ma  
421 chemical weathering displayed by both 3710-3700 Ma volcano-sedimentary rocks  
422 (Nutman *et al.*, 2012a) and by  $\geq 3710$  igneous rocks (Fig. 5). As demonstrated by  
423 Nesbitt *et al.* (1997), *highly variable* degrees of weathering within a single terrane are  
424 indicative of tectonic instability.

425

#### 426 *Apparent sea level*

427 All of the early ( $\geq 3710$  Ma) mafic to intermediate volcanic rocks, preserved in  
428 rare low strain zones have relict pillow structures (Nutman *et al.*, 1984; Komiya *et al.*,  
429 1999; Solvang, 1999; Furnes *et al.*, 2007). Thus early volcanism was all submarine.  
430 3710-3700 Ma felsic and mafic volcano-sedimentary rocks display variable and locally  
431 intense weathering, indication of emergence of the source regions (Nutman *et al.*,  
432 2012a). Likewise, it is demonstrated here that *c.* 3710 Ma pillowed volcanic rocks  
433 were strongly weathered, prior to deposition on top of them of 3695-3690 Ma chemical  
434 sedimentary rocks. This shows emergence, followed a transgression between  
435 3710-3695 Ma. Therefore, throughout the  $\geq 3720$  Ma-3690 Ma evolution of the  
436 supracrustal assemblage there were changes in relative sea level. These apparent sea  
437 level changes can be because of progressive accumulation of the igneous suites so that  
438 they eventually emerged above sea level. However, syn-igneous tectonic thickening of  
439 the crust was at least partly responsible for the emergence, as demonstrated by  $\geq 3717$



440 Ma tectonic intercalation of upper mantle dunites and harzburgites within crustal  
441 sequences (Fig. 2; Friend & Nutman, 2010, 2011). However after the emergence, there  
442 was clearly a transgression followed by the deposition of chemical sedimentary rocks,  
443 indicating a relative rise in sea level between 3710-3695 Ma.

444

#### 445 *Comparison with Phanerozoic intra-oceanic arc and plateau settings*

446 Because the *c.* 3700 Ma Isua assemblage consists of essentially juvenile crust at  
447 the time it formed, two possible settings for its formation are at an intra-oceanic  
448 convergent plate boundary and within an intra-oceanic mafic plateau. The integrated  
449 data set allows clear discrimination between these possibilities. The  $\geq 3720$ -3690 Ma  
450 igneous activity took place in a tectonically active setting, with tectonic intercalation of  
451 crustal and mantle rocks *during* the development of the package, not just in  
452 superimposed, younger, unrelated, tectonic events. This crust mantle intercalation  
453 would not be observed during the development of an intra-oceanic plateau, distal from  
454 convergent plate boundaries, but it does occur at intra-oceanic convergent plate  
455 boundaries (Shervais, 2001 and references therein). Geochemically, there is a temporal  
456 shift from mafic, to intermediate and then felsic igneous rocks (Nutman & Friend,  
457 2009). The earlier mafic-intermediate igneous suites ( $\geq 3720$ -3710 Ma) have  
458 geochemical signatures indicating melting of depleted mantle by fluid fluxing (Polat *et*  
459 *al.*, 2002; Polat & Hofmann, 2003; Hoffmann *et al.*, 2011b and data in this paper). The  
460 younger 3700-3690 Ma tonalites on the north side of the belt are classic Archaean  
461 calc-alkaline rocks, with geochemical signatures indicating melting of high pressure  
462 (garnetiferous) mafic rocks. Calc-alkaline magmatism appears with the maturing of  
463 intra-oceanic island arcs (e.g. Shervais, 2001). On the other hand, adiabatic  
464 decompression dry melting in mantle diapirs is the essential processes in the formation  
465 of most igneous rocks in intra-oceanic within-plate settings (Farnetani & Richards,  
466 1994 and references therein).

467 Based then on geochemical criteria, the *c.* 3700 Ma Isua assemblage has  
468 characteristics expected at convergent plate boundary settings and shows many of the  
469 features recognised in the birth, death and resurrection life cycle of suprasubduction  
470 zone ophiolites (arc assemblages; Dilek & Polat, 2008; Friend & Nutman, 2010). As  
471 summarised by Stern & Bloomer (1992) and Shervais (2001), key features of this cycle  
472 as seen in *c.* 3700 Ma Isua are: Tectonically active, with early mafic rocks produced  
473 from the upper mantle by fluid fluxing and melt overprinting from the 'subducted' slab

474 to produce submarine boninites and arc basalts, then subaerial emergence with the  
475 transition of magmas towards more felsic calc-alkaline varieties and the production of  
476 felsic volcano-sedimentary and sedimentary aprons from the emergent volcanic  
477 centres.

478

479 *Eoarchaean 'proto-arcs' based on Isua crust formation at c. 3700 Ma*

480 It is likely that the internal architecture of Eoarchaean intra-oceanic island arcs  
481 was markedly different from those in the Phanerozoic, albeit geodynamically they  
482 occupied the same niche; *i.e.* the removal of 'excess' oceanic first-generation crust  
483 from Earth's surface by the formation of second-generation intermediate to felsic  
484 juvenile crust. For these Eoarchaean arc-like features we here introduce the term  
485 '*proto-arcs*' – to stress that they might have had an architecture very different from  
486 modern arc systems. One marked difference could have been the lack of a discrete,  
487 long-lived single subduction zone to transport oceanic crust well below the  
488 asthenosphere. Instead, mature proto-arcs might have been marked by imbricate  
489 packages of intercalated oceanic crust, uppermost mantle and earliest mafic proto-arc  
490 crust, that extended only into the uppermost mantle (de Wit, 1986; Nutman *et al.*,  
491 2007; Nagel *et al.*, 2012).

492 The different thermal state of the Eoarchaean Earth is why *c.* 3700 Ma  
493 convergent plate boundaries were unlikely to be the same as modern intra-oceanic  
494 subduction channel + arc assemblages. One important factor to consider is the relative  
495 buoyancy of 'oceanic' mafic crust versus the asthenosphere. On the modern Earth,  
496 subduction continues because older, cold oceanic crust becomes denser than the  
497 asthenosphere, and upon rupture will sink through it. Thus it is widely recognised that  
498 during the life of intra-oceanic subduction systems, the conserved plate is mostly under  
499 tension, commonly with the roll-back of the subduction zone (Collins, 2002; Cawood,  
500 2005). With time, in modern systems that are not sediment starved, this will lead to the  
501 overstepping of the fore-arc volcanic apron by younger arc igneous rocks (e.g.,  
502 Cawood *et al.*, 2011 and references therein). If in the Eoarchaean the oceanic crust  
503 typically remained buoyant relative to the asthenosphere (because oceanic crust was  
504 hotter? younger?) then the commonest style of Phanerozoic intra-oceanic subduction  
505 could not operate. However, in order to compensate for oceanic crust production along  
506 spreading centres, Eoarchaean convergent plate boundaries must have existed. An  
507 initial compressional intra-oceanic rupture zone would have intercalated mantle with

508 still-buoyant oceanic crust. At the earliest stage of proto-arc development (this stage is  
509 *not* illustrated in Fig. 8), this would have promoted the formation of magmas by  
510 fluid-fluxing of the upper mantle to produce the Eoarchaeon equivalents of the  
511 boninites and arc tholeiites, as seen in the earliest stages of Phanerozoic intra-oceanic  
512 arc development (Sterner & Bloomer, 1992; Shervais, 2001). Thereafter, the buoyancy  
513 of the underthrust oceanic crust would have promoted a compressional tectonic  
514 regime, because of the inability of that crust to undergo Phanerozoic-style subduction  
515 (*i.e.*, sink into the mantle on its own accord). Crustal shortening in this compressional  
516 regime would have been accommodated by tectonic intercalation (Fig. 8A; e.g. deWitt,  
517 1985; Nutman *et al.*, 2007). Pressure increase at the base of this growing imbricated  
518 pile combined with temperature increase by conduction would have caused melting  
519 first in the stability field of garnet amphibolite (and/or high pressure granulite) and  
520 then rutile-bearing eclogite (Hoffmann *et al.*, 2011a). This temporal progression in  
521 changing geochemistry is in keeping with garnet-signatures only being present in the  
522 youngest rocks of the *c.* 3700 Ma Isua assemblage – the 3700-3690 Ma high SiO<sub>2</sub> –  
523 low MgO tonalites, which display trace element signatures such as high La/Yb<sub>(N)</sub> and  
524 low Yb<sub>(N)</sub> (Fig. 7C).

525 Another feature of this model is that the earliest proto-arc components – largely  
526 mafic volcanic rocks, gabbros with intercalations of upper mantle rocks – were  
527 preserved in the crust by being locked in a greater volume of more silicic rocks formed  
528 by the melting of underthrust eclogitised mafic crust. Thus in the prot-arc model,  
529 oceanic (MORB-like) crust will have a much lower crustal preservation potential than  
530 the early mafic arc rocks. This is because there is a much greater probability of it being  
531 partially melted at depth to produce garnetiferous restites that remain in the mantle,  
532 than for it being tectonically emplaced and preserved into the crust. No doubt this  
533 genre of model will require further testing, but at present it satisfies not only  
534 geochemical and isotopic constraints, but geochronological and structural geology  
535 ones as well.

536 An important difference between Archaean proto-arcs and modern arc systems  
537 would have been the bias between different melting mechanisms (Martin, 1986).  
538 Although the melting of eclogitised slab does occur locally on Earth today, recycling of  
539 oceanic crust into the deep mantle with fluid-loss is a much more important process.  
540 For this reason Phanerozoic island arc magmatism produces largely basaltic-andesitic  
541 suites, with lesser amounts of more silicic rocks. In the Phanerozoic, the production of

542 more silicic compositions is predominantly in continental arcs, where the silicic  
543 compositions show isotopic evidence of recycling of the older continental rocks (e.g.,  
544 Hildreth & Moorbath, 1988). However, in the Eoarchaeon, the greater importance of  
545 melting of mafic eclogite led to silicic rocks such as tonalites being the dominant  
546 product of proto-arc magmatism, with only lesser amounts of slightly older basalts and  
547 andesites preserved as enclaves and tectonic slices within them. Hence in contrast to  
548 Phanerozoic silicic arc magmas, those formed in the Eoarchaeon are predominantly  
549 juvenile additions to the crust, and therefore contributing to net growth of the crust  
550 more effectively.

551

552

553 *Eoarchaean proto-arcs and mantle isotopic signatures*

554 It is increasingly recognized that there is a change in the pattern of  $^{143}\text{Nd}$   
555 and  $^{176}\text{Hf}$  isotopic evolution in the mantle, as reflected in the isotopic signatures of  
556 Archaean juvenile granitoids and mantle-derived rocks, with an inflection in both  
557 long-lived systems occurring between 3600 Ma and 3200 Ma (c.f., Bennett *et al.*,  
558 1993, Hiess *et al.*, 2009, Næraa *et al.*, 2012). Pre-3500 Ma, mantle derived samples are  
559 characterised by near chondritic  $\epsilon_{\text{Hf}}$  and positive  $\epsilon_{\text{Nd}}$  values. Post 3200 Ma, both  
560 systems are characterized by a quasi-linear evolution with a well defined correlation of  
561 positive  $\epsilon_{\text{Hf}}$  and  $\epsilon_{\text{Nd}}$  values (Vervoort *et al.*, 2011).

562 The near chondritic Eoarchaean  $\epsilon_{\text{Hf}}$  compositions likely reflect the limited  
563 extent of Hadean and early Archaean crust and thus its minimal impact on mantle  
564 isotopic evolution, but may also be related changes in arc processes. As previously  
565 discussed, the chemistry of the basalts must at least in part reflect depleted mantle  
566 overprinted by subduction components. During the proto-arc era and in contrast to  
567 younger time periods, any subducted sediments contributing to Isua arc development  
568 were likely of similar Hf and Nd isotopic composition to the mantle. Although Sm and  
569 Nd and to a lesser extent Lu and Hf can be fractionated by subduction fluids and melts,  
570 there was insufficient time to generate significant isotopic variations in the  
571 sedimentary component prior to subduction. Furthermore, the efficacy of crustal  
572 extraction and mixing of depleted mantle domains might have been hindered by the  
573 lack of well-developed, subduction systems resulting in slower transfer and  
574 homogenisation of isotopic signatures into the upper mantle.

575 A significant difference between Eoarchaean proto-arcs versus younger arc  
576 systems, is the widespread partial melting of recycled mafic crust, giving rise to  
577 distinctive Archean tonalite-trondhjemite-granodiorite suites and resulting in the  
578 formation of extensive garnet  $\pm$  clinopyroxene (with very high Lu/Hf and high Sm/Nd)  
579 restites in the upper mantle (Nutman *et al.*, 1999). These restites would develop highly  
580 radiogenic Hf and Nd isotopic compositions. The behavior of these residues in the  
581 Archean mantle, and their possible influence on mantle isotope characteristics have  
582 been little considered. Here we speculate that in the Archaean, refractory residues from  
583 TTG genesis may have been resistant to mixing in the upper mantle. If this were the  
584 case, the storage of these garnetiferous residues would result in delaying the depletion  
585 of Lu/Hf and Sm/Nd and as such buffering upper mantle Nd and Hf isotopic

586 signatures. Although melting of such restites directly would not produce boninitic  
587 composition melts, we further note that *c.* 3900 Ma restites (complementary to the  
588 oldest Itsaq Gneiss Complex tonalites) could generate a mantle source with the  
589 distinctive radiogenic  $\epsilon_{\text{Hf}}$  and  $\epsilon_{\text{Nd}}$  characteristics noted for the  $\geq 3720$  Ma Isua boninites  
590 by Hoffmann *et al.* (2010).

591

## 592 **Conclusions**

593 (1) The 3720-3690 Ma isotopically juvenile crustal assemblage at Isua shows a  
594 progression from mafic to felsic combined with geochemical signatures indicating  
595 generation initially by fluid fluxing  $\pm$  melt transport through the depleted upper mantle  
596 succeeded by partial melting of garnetiferous metamorphosed mafic rocks.

597 (2) Within the 3720-3690 Ma period there was tectonic intercalation of crustal and  
598 mantle rocks, indicating a tectonically-active environment *during* crust formation.

599 (3) Tectonic activity juxtaposed rocks ranging in age from  $\geq 3720$  Ma to 3690 Ma, that  
600 had formed in different environments ranging from deep to shallow water and  
601 subaerial.

602 (4) The geochemical characteristics of the 3720-3690 Ma syn-tectonic Isua assemblage  
603 show melting mechanisms known in post-Archaeon arc settings, and are best viewed  
604 as ‘proto-arcs’ having formed along Eoarchaeon convergent plate boundaries.

605 (5) The Eoarchaeon proto-arcs had the same geodynamic function as arcs today, i.e. the  
606 ‘disposal’ of oceanic crust production coupled with the formation of buoyant  
607 intermediate-felsic crust. In our evolving working model, we suggest that their tectonic  
608 architecture was likely different from modern arcs, with broad crustal imbrication  
609 zones without mass transfer below the asthenosphere, i.e., lacking a discrete  
610 subduction zone recycling oceanic crust below the upper mantle.

611

## 612 **Acknowledgements**

613 Research was supported by ARC grant DP120100273. Ole Christiansen of Nunamineral A/S is  
614 thanked for logistical support.

## 615 **References**

616 ALLAART, J.H. 1976. The pre-3760 m.y. old supracrustal rocks of the Isua area, central West  
617 Greenland, and the associated occurrence of quartz-banded ironstone. *In*: WINDLEY,  
618 B.F. (ed), *The Early History of the Earth*. Wiley, London, pp. 177-189.

- 619 BAADSGAARD, H., NUTMAN, A.P. & BRIDGWATER, D. 1986a. Geochronology and isotope  
620 geochemistry of the early Archaean Amîtsoq gneisses of the Isukasia area, southern  
621 West Greenland. *Geochimica et Cosmochimica Acta*, **50**, 2173-2183.
- 622 BAADSGAARD, H., NUTMAN, A.P., ROSING, M., BRIDGWATER, D. & LONGSTAFFE, F.J.  
623 1986b. Alteration and metamorphism of Amîtsoq gneisses from the Isukasia area, West  
624 Greenland: Recommendations for isotope studies of the early crust. *Geochimica et*  
625 *Cosmochimica Acta*, **50**, 2165-2172.
- 626 BENNETT, V.C., NUTMAN, A.P. & McCULLOCH, M.T. 1993. Nd isotopic evidence for  
627 transient, highly depleted mantle reservoirs in the early history of the Earth. *Earth and*  
628 *Planetary Science Letters*, **119**, 299-317.
- 629 BENNETT, V.C., NUTMAN, A.P. & ESAT, T.M. 2003. Constraints on mantle evolution and  
630 differentiation from  $^{187}\text{Os}/^{188}\text{Os}$  isotopic compositions of Archaean ultramafic rocks  
631 from southern West Greenland (3.8 Ga) and Western Australia (3.45 Ga). *Geochimica*  
632 *et Cosmochimica Acta*, **66**, 2615-2630.
- 633 BENNETT V. C., BRANDON, A.D. & NUTMAN, A.P. 2007. Hadean mantle dynamics from  
634 coupled 142-143 neodymium isotopes in Eoarchaeon rocks. *Science*, **318**, 1907-1910.
- 635 BOHLAR, R., KAMBER, B.S., MOORBATH, S., FEDO, C.M. & WHITEHOUSE, M.J. 2004.  
636 Characterisation of early Archaean chemical sediments by trace element signatures.  
637 *Earth and Planetary Science Letters*, **222**, 43-60.
- 638 BOHLAR, R., KAMBER, B. S., MOORBATH, S., WHITEHOUSE, M. J. & COLLERSON, K.  
639 D. 2005. Chemical characterization of earth's most ancient clastic  
640 metasediments from Isua. *Geochimica et Cosmochimica Acta*, **69**, 1553-1573.
- 641 BOWRING, S. & WILLIAMS, I. S. 1999. Priscoan (4.00-4.03 Ga) orthogneisses from  
642 northwestern Canada. *Contributions to Mineralogy and Petrology*, **134**, 3-16.
- 643 CARO, G., BOURDON, B., WOOD, B.J. & CORGNE, A. 2005. Trace element  
644 fractionation in the Hadean mantle generated by melt segregation from a magma  
645 ocean. *Nature*, **434**, 246-249.
- 646 CAWOOD, P.A. 2005. Terra Australia orogen: Rodinia breakup and development of the  
647 Pacific and Iapetus margins of Gondwana during the Neoproterozoic and  
648 Paleozoic. *Earth-Science Reviews*, **69**, 249-279.
- 649 CAWOOD, P.A., LEITCH, E.C., MERLE, R.E. & NEMCHIN, A.A. 2011. Orogenesis without  
650 collision: Stabilizing the Terra Australia accretionary orogen, eastern Australia.  
651 *Geological Society of America Bulletin* doi:10.1130/B30415.1

- 652 COLLERSON, K.D., CAMPBELL L.M., WEAVER, B.L. & PALACZ, Z.A. 1991. Evidence for  
653 extreme mantle fractionation in early Archaean ultramafic rocks from northern  
654 Labrador. *Nature*, **349**, 209-214.
- 655 COLLINS, W.J. 2002. Nature of extensional accretionary orogens. *Tectonics*, **21**, 6-1-6-12.
- 656 CRADDOCK, P.R. & DAUPHAS, N. 2011. Iron and carbon isotope evidence for microbial iron  
657 respiration throughout the Archean. *Earth and Planetary Science Letters*, **303**,  
658 121–132.
- 659 CROWLEY, J.L. 2002. Testing the model of late Archean terrane accretion in southern West  
660 Greenland: a comparison of timing of geological events across the Qarliit Nunaat fault,  
661 Buksefjorden region. *Precambrian Research*, **116**, 57-79.
- 662 CROWLEY, J.L. 2003. U-Pb geochronology of 3810-3630 Ma granitoid rocks south of the  
663 Isua greenstone belt, southern West Greenland. *Precambrian Research*, **126**, 235-257.
- 664 CROWLEY, J.L., MYERS, J.S. & DUNNING, G.R. 2002. The timing and nature of multiple  
665 3700-3600 Ma tectonic events in granitoid rocks north of the Isua greenstone belt,  
666 southern West Greenland. *Geological Society of America Bulletin*, **114**, 1311-1325.
- 667 DAUPHAS, N., VAN ZUILEN, M., WADHWA, M., DAVIS, A.M., MARTY, B. & JANNEY, P.E.  
668 2004. Clues from Fe isotope variations on the origin of early Archean BIFs from  
669 Greenland. *Science*, **306**, 2077-2080.
- 670 DHUMIE, B., HAWKESWORTH, C.J., CAWOOD, P.A. & STOREY, C.D. 2012. A change in the  
671 geodynamics of continental growth 3 billion years ago. *Science*, **335**, 134-1336.
- 672 DE WIT, M.J. 1986. What the oldest rocks say. In: ASHWAL, L., BURKE, K., de WIT, M. &  
673 WELLS, G. (eds.) *The Earth as a Planet*. LPI Technical Report 86-08, Lunar and  
674 Planetary Institute, Houston, Texas.
- 675 DILEK, Y., POLAT, A. 2008. Suprasubduction zone ophiolites and Archean tectonics.  
676 *Geology*, **36**, 431-432.
- 677 DYMEK, R.F., BROTHERS, S.C. & SCHIFFRIES, C.M. 1988. Petrogenesis of ultramafic  
678 metamorphic rocks from the 3800 Ma Isua supracrustal belt, West Greenland.  
679 *Journal of Petrology*, **29**, 1353-1397.
- 680 EGGINS, S.M. 1993. Origin and differentiation of picritic arc magmas, Ambae(Aoba),  
681 Vanuatu. *Contributions to Mineralogy and Petrology*, **114**, 79-100.
- 682 FARNETANI, C.G. & RICHARDS, A.A. 1994. Numerical investigations of the mantle  
683 plume initiation model for flood basalt events. *Journal of Geophysical Research*,  
684 **99**, 13813-13833.



- 685 FRIEND, C.R.L. & NUTMAN, A.P. 2005a. Complex 3670-3500 Ma orogenic episodes  
686 superimposed on juvenile crust accreted between 3850-3690 Ma, Itsaq Gneiss  
687 Complex, southern West Greenland. *Journal of Geology*, **113**, 375-398.
- 688 FRIEND, C.R.L. & NUTMAN, A.P. 2005b. New pieces to the Archaean terrane jigsaw puzzle  
689 in the Nuuk region, southern West Greenland: Steps in transforming a simple insight  
690 into a complex regional tectonothermal model. *Journal of the Geological Society of  
691 London*, **162**, 147-163.
- 692 FRIEND, C.R.L. & NUTMAN, A.P. 2010. Eoarchean ophiolites? New evidence for the debate  
693 on the Isua supracrustal belt, southern West Greenland. *American Journal of Science*,  
694 **310**, 826-861.
- 695 FRIEND, C.R.L. & NUTMAN, A.P. 2011. Dunites from Isua, southern West Greenland: A ca.  
696 3720 Ma window into subcrustal metasomatism of depleted mantle. *Geology*, **39**,  
697 663-666.
- 698 FRIEND, C.R.L., BENNETT, V.C. & NUTMAN, A.P. 2002. Abyssal peridotites >3,800 Ma  
699 from southern West Greenland: field relationships, petrography, geochronology,  
700 whole-rock and mineral chemistry of dunite and harzburgite inclusions in the Itsaq  
701 Gneiss Complex. *Contributions to Mineralogy and Petrology*, **143**, 71-92.
- 702 FRIEND, C.R.L., NUTMAN, A.P. & MCGREGOR, V.R. 1987. Late-Archaean tectonics in the  
703 Færingehavn - Tre Brødre area, south of Buksefjorden, southern West Greenland.  
704 *Journal of the Geological Society of London*, **144**, 369-376.
- 705 FRIEND, C.R.L., BENNETT, V.C., NUTMAN, A.P. & NORMAN, M.D. 2007. Seawater trace  
706 element signatures (REE+Y) from Eoarchean chemical (meta)sedimentary rocks,  
707 southern West Greenland *Contributions to Mineralogy and Petrology*, **155**, 229-246,  
708 DOI 10.1007/S00410-007-0239-z.
- 709 FRIEND, C.R.L., NUTMAN, A.P. & MCGREGOR, V.R. 1988. Late Archaean terrane accretion  
710 in the Godthåb region, southern West Greenland. *Nature*, **335**, 535-538.
- 711 FURNES, H., de WIT, M., STAUDIGEL, H., ROSING, M. & MUEHLENBACHS, K. 2007. A  
712 vestige of Earth's oldest ophiolite. *Science*, **215**, 1704-1707.
- 713 FURNES, H., ROSING, M., DILEK, Y. & de WIT, M. 2009. Isua supracrustal belt (Greenland) –  
714 a vestige of a 3.8 Ga suprasubduction zone ophiolite, and the implications for Archaean  
715 geology. *Lithos*, **113**, 115-132.
- 716 GILL, R.C.O., BRIDGWATER, D. & ALLAART, J.H. 1981. The geochemistry of the earliest  
717 known basic metavolcanic rocks at Isua, West Greenland: A preliminary investigation.  
718 *Special Publication of the Geological Society of Australia*, **7**, 313-325.

- 719 GRIFFIN, W.L., MCGREGOR, V.R., NUTMAN, A.P., TAYLOR, P.N. & BRIDGWATER, D. 1980.  
720 Early Archaean granulite-facies metamorphism south of Amealik. *Earth and*  
721 *Planetary Science Letters*, **50**, 59-74.
- 722 HAMILTON, P.J., O'NIONS, R.K., EVENSEN, N.H., BRIDGWATER, D. & ALLAART, J.H.  
723 1978. Sm-Nd isotopic investigations of Isua supracrustals and implications for mantle  
724 evolution. *Nature*, **272**, 41-43.
- 725 HIESS, J., BENNETT, V.C., NUTMAN, A.P. & WILLIAMS, I.S. 2009. In situ U–Pb, O and Hf  
726 isotopic compositions of zircon and olivine from Eoarchean rocks, West Greenland:  
727 New insights to making old crust. *Geochimica et Cosmochimica Acta*, **73**, 4489–4516.
- 728 HILDRETH, W. & MOORBATH, S. 1988. Crustal contributions to arc magmatism in the Andes  
729 of Central Chile. *Contributions to Mineralogy and Petrology*, **98**, 455-489.
- 730 HOFFMANN, J.E., MÜNKER, C., POLAT, A., KONIG, S., MEZGER, K. & ROSING, M.T. 2010.  
731 Highly depleted Hadean mantle reservoirs in the sources of early Archean arc-like  
732 rocks, Isua supracrustal belt, southern West Greenland. *Geochimica et Cosmochimica*  
733 *Acta*, **74**, 7236-7260.
- 734 HOFFMANN, J.E., MÜNKER, C., NÆRAA, T. & ROSING, M.T. 2011a. Mechanisms of Archean  
735 crust formation inferred from high-precision HFSE systematics in TTGs. *Geochimica*  
736 *et Cosmochimica Acta*, **75**, 4157-4178.
- 737 HOFFMANN, J.E., MÜNKER, C., POLAT, A., ROSING, M.T. & SCHULZ, T. 2011b. The origin  
738 of decoupled Hf-Nd isotope compositions in Eoarchean rocks from southern West  
739 Greenland. *Geochimica et Cosmochimica Acta*, **75**, 6610-6628.
- 740 HORIE, K., NUTMAN, A.P., FRIEND, C.R.L. & HIDAKA, H. 2010. The complex age of  
741 orthogneiss protoliths exemplified by the Eoarchean Itsaq Gneiss Complex (Greenland):  
742 SHRIMP and old rocks. *Precambrian Research*, **181**, 25-43.
- 743 IIZUKA, T., KOMIYA, T., UENO, Y., KATAYAMA, I., UEHARA, Y., MARUYAMA, S.,  
744 HIRATA, T., JOHNSON, S.P. & DUNKLEY, D.J. 2007. Geology and zircon  
745 geochronology of the Acasta Gneiss Complex, northwestern Canada: New constraints  
746 on its tectonothermal history. *Precambrian Research*, **153**, 179–208.
- 747 JACOBSEN, S.B. & DYMEK, R.F. 1987. Nd and Sr isotope systematics of clastic  
748 metasediments from Isua, West Greenland: Identification of pre-3.8 Ga differentiated  
749 crustal components. *Journal of Geophysical Research*, **93**, 338-354.
- 750 JENNER, F.E., BENNETT, V.C., NUTMAN, A.P., FRIEND, C.R.L., NORMAN, M.D. &  
751 YAXLEY, G. 2009. Evidence for subduction at 3.8 Ga: Geochemistry of arc-like  
752 metabasalts from the southern edge of the Isua Supracrustal Belt. *Chemical*

- 753 *Geology*, **261**, 82-99.
- 754 KAMBER, B.S., WHITEHOUSE, M.J., BOLHAR, R. & MOORBATH, S. 2005. Volcanic  
755 resurfacing and the early terrestrial crust: Zircon U-Pb and REE constraints from the  
756 Isua Greenstone Belt, southern West Greenland. *Earth and Planetary Science Letters*,  
757 **240**, 276-290.
- 758 KINNY, P.D. & NUTMAN, A.P. 1996. Zirconology of the Meeberrie gneiss, Yilgarn Craton,  
759 Western Australia: an early Archaean migmatite. *Precambrian Research*, **78**, 165-178.
- 760 KOMIYA, T., MARUYAMA, S., MASUDA, T., APPEL, P.W.U. & NOHDA, S. 1999. The 3.8-3.7  
761 Ga plate tectonics on the Earth; Field evidence from the Isua accretionary complex,  
762 West Greenland: *Journal of Geology*, **107**, 515-554.
- 763 LIU, D., WAN, Y., WU, J.S., WILDE, S.A., ZHOU, H.Y., DONG, C.Y., & YIN, X.Y. 2007.  
764 Eoarchean rocks and zircons in the North China Craton. In: VAN KRANENDONK, M.J.,  
765 SMITHIES, R.H., & BENNETT, V.C. (eds) *Earth's Oldest Rocks*. Elsevier, pp. 251-274.
- 766 MARTIN, H. 1986. Effect of steeper Archaean geothermal gradient on geochemistry of  
767 subduction-zone magmas. *Geology*, **14**, 753-756.
- 768 MACPHERSON, C.G., DREHER, S.T. & THIRLWALL, M.F. 2006. Adakites without slab  
769 melting: High pressure differentiation of island arc magma, Mindanao, the Philippines.  
770 *Earth and Planetary Science Letters*, **243**, 581-593.
- 771 MARTIN, H. SMITHIES, R.H., RAPP, R., MOYEN, J.-F. & CHAMPION, D. 2005. An overview  
772 of adakite, tonalite-trondhjemite-granodiorite (TTG), and sanukitoid: relationships and  
773 some implications for crustal evolution. *Lithos*, **79**, 1-24.
- 774 MCGREGOR, V.R. 1973. The early Precambrian gneisses of the Godthåb district, West  
775 Greenland. *Philosophical Transactions of the Royal Society of London*, **A273**,  
776 343-358.
- 777 MOORBATH, S. 1975. Evolution of Precambrian crust from strontium isotopic evidence.  
778 *Nature*, **254**, 395-398.
- 779 MOORBATH, S., O'NIONS, R.K. & PANKHURST, R.J. 1973. Early Archaean age for the Isua  
780 iron formation, West Greenland. *Nature*, **245**, 138-139.
- 781 MOORBATH, S., O'NIONS, R.K., PANKHURST, R.J., GALE, N.H. & MCGREGOR, V.R. 1972.  
782 Further rubidium-strontium age determinations on the very early Precambrian rocks of  
783 the Godthåb district: West Greenland. *Nature*, **240**, 78-82.
- 784 MOORBATH, S., ALLAART, J.H., BRIDGWATER, D. & MCGREGOR, V.R. 1977. Rb-Sr ages of  
785 early Archaean supracrustal rocks and Amîtsoq gneisses at Isua. *Nature*, **270**, 43-45.

- 786 MOORBATH, S. 2005. Oldest rocks, earliest life, heaviest impacts, and the Hadean–Archaean  
787 transition. *Applied Geochemistry*, **20**, 819–824.
- 788 MYERS, J.S. 2001. Protoliths of the 3.8–3.7 Ga Isua greenstone belt, West Greenland.  
789 *Precambrian Research*, **105**, 129-141.
- 790 NAGEL, T.J., HOFFMANN, J.E., MÜNKER, C. 2012. Generation of Eoarchean  
791 tonalite-trondhjemite-granodiorite series from thickened mafic arc crust. *Geology*, doi:  
792 10.1130/G32729.1
- 793 NÆRAA, T., SCHERSTÉN, ROSING, M.T., KEMP, A.I.S., HOFFMANN, J.E., KOKFELT, T.F.,  
794 WHITEHOUSE, M.J. 2012. Hafnium isotope evidence for a transition in the dynamics of  
795 continental growth 3.2 Gyr ago. *Nature*, **485**, 627-631.
- 796 NESBITT, H.W., FEDO, C.M. & YOUNG, G.G. 1997. Quartz and feldspar stability, steady and  
797 non-steady-state weathering, and petrogenesis of siliciclastic sands and muds. *Journal*  
798 *of Geology*, **105**, 173-191.
- 799 NUTMAN, A.P. 1984. Early Archaean crustal evolution of the Isukasia area, southern West  
800 Greenland. In: Kröner, A. & Greiling, R. (eds) *Precambrian Tectonics Illustrated*.  
801 Stuttgart, E. Schweizerbart'sche Verlagsbuchhandlung.
- 802 NUTMAN, A.P. 2006. Antiquity of the Oceans and Continents. *Elements*, **2**, 223-227.
- 803 NUTMAN, A.P. & BRIDGWATER, D. 1986. Early Archaean Amîtsoq tonalites and granites  
804 from the Isukasia area, southern West Greenland: Development of the oldest-known  
805 sial. *Contributions to Mineralogy and Petrology*, **94**, 137-148.
- 806 NUTMAN, A.P. & FRIEND, C.R.L. 2007. Terranes with ca. 2715 and 2650 Ma high-pressure  
807 metamorphisms juxtaposed in the Nuuk region, southern West Greenland:  
808 Complexities of Neoarchean collisional orogeny. *Precambrian Research*, **155**,  
809 159-203.
- 810 NUTMAN, A.P. & FRIEND, C.R.L. 2009. New 1:20000 geological maps, synthesis and  
811 history of the Isua supracrustal belt and adjacent gneisses, Nuuk region, southern  
812 West Greenland: A glimpse of Eoarchean crust formation and orogeny.  
813 *Precambrian Research*, **172**, 189-211.
- 814 NUTMAN, A.P., FRIEND, C.R.L. & BENNETT, V.C., 2002b. Evidence for 3650-3600  
815 Ma assembly of the northern end of the Itsaq Gneiss Complex, Greenland:  
816 Implication for early Archean tectonics. *Tectonics*, **21**, article 5
- 817 NUTMAN, A.P., FRIEND, C.R.L. & PAXTON, S. 2009. Detrital zircon sedimentary  
818 provenance ages for the Eoarchean Isua supracrustal belt southern West  
819 Greenland: Juxtaposition of ca. 3700 Ma juvenile arc assemblages against an

- 820 older complex with 3920-3800 Ma components: *Precambrian Research*, **172**,  
821 212-233.
- 822 NUTMAN, A.P., ALLAART, J.H., BRIDGWATER, D. DIMROTH, E. & ROSING, M.T. 1984.  
823 Stratigraphic and geochemical evidence for the depositional environment of the early  
824 Archaean Isua supracrustal belt, southern West Greenland. *Precambrian Research*, **25**,  
825 365-396.
- 826 NUTMAN, A.P., KINNY, P.D., COMPSTON, W. & WILLIAMS, I.S. 1991. SHRIMP U-Pb  
827 zircon geochronology of the Narryer Gneiss Complex, Western Australia:  
828 *Precambrian Research*, **52**, 275-300.
- 829 NUTMAN, A.P., MCGREGOR, V.R., FRIEND, C.R.L., BENNETT, V.C. & KINNY, P.D. 1996.  
830 The Itsaq Gneiss Complex of southern West Greenland; the world's most extensive  
831 record of early crustal evolution (3900-3600 Ma). *Precambrian Research*, **78**, 1-39.
- 832 NUTMAN, A.P., BENNETT, V.C., FRIEND, C.R.L. & ROSING, M.T. 1997. ~3710 and  $\geq 3790$   
833 Ma volcanic sequences in the Isua (Greenland) supracrustal belt; structural and Nd  
834 isotope implications. *Chemical Geology*, **141**, 271-287.
- 835 NUTMAN, A.P., BENNETT, V.C., FRIEND, C.R.L. & NORMAN, M. 1999. Meta-igneous  
836 (non-gneissic) tonalites and quartz-diorites from an extensive ca. 3800 Ma terrain south  
837 of the Isua supracrustal belt, southern West Greenland: constraints on early crust  
838 formation. *Contributions to Mineralogy and Petrology*, **137**, 364-388.
- 839 NUTMAN, A.P., FRIEND, C.R.L., BENNETT, V.C. & MCGREGOR, V.R. 2000. The early  
840 Archaean Itsaq Gneiss Complex of southern West Greenland: The importance of field  
841 observations in interpreting dates and isotopic data constraining early terrestrial  
842 evolution. *Geochimica et Cosmochimica Acta*, **64**, 3035-3060.
- 843 NUTMAN, A.P., FRIEND, C.R.L. & BENNETT, V.C. 2002. Evidence for 3650-3600 Ma  
844 assembly of the northern end of the Itsaq Gneiss Complex, Greenland: Implication for  
845 early Archean tectonics. *Tectonics*, **21**, article 5
- 846 NUTMAN, A.P., FRIEND, C.R.L., HORIE, H. & HIDAKA, H. 2007. Construction of pre-3600  
847 Ma crust at convergent plate boundaries, exemplified by the Itsaq Gneiss Complex of  
848 southern West Greenland. In: van Kranendonk, M. J., Smithies, R. H., and Bennett,  
849 V.C. (eds) *Earth's Oldest Rocks*. Elsevier, p.187-218.
- 850 NUTMAN, A.P., FRIEND, C.R.L., BENNETT, V.C., WRIGHT, D. & NORMAN, M.D. 2010.  
851  $\geq 3700$  Ma pre-metamorphic dolomite formed by microbial mediation in the Isua  
852 supracrustal belt (W Greenland). Simple evidence for early life? *Precambrian*  
853 *Research*, **183**, 725-737.

- 854 NUTMAN, A.P., BENNETT, V.C., FRIEND, C.R.L. 2012a. Waves and weathering at 3.7 Ga:  
855 Geologic evidence for an equitable climate under the faint early Sun. *Australian*  
856 *Journal of Earth Sciences*, DOI:10.1080/08120099.2012.618512.
- 857 NUTMAN, A.P., BENNETT, V.C., FRIEND, C.R.L., HIESS, J., YI, K., LEE, S.R., 2012b.  
858 Making and breaking the oldest crust – Greenland’s 3.9-3.6 Ga Itsaq Gneiss Complex:  
859 Quantum-tectonics juvenile crustal growth followed by recycling during post-collisional  
860 crustal extension. 34<sup>th</sup> International Geological Congress (Brisbane) abstracts.
- 861 OHATA, T. & ARAI, H. 2007. Statistical empirical index to chemical weathering in igneous  
862 rocks: A new tool for evaluating the degree of weathering. *Chemical Geology*, **240**,  
863 280-297.
- 864 O’NEIL, J., MAURICE, C., STEVENSON, R.K., LAROCQUE, J., CLOQUET, C., DAVID, J. &  
865 FRANCIS, D. 2007. The geology of the 3.8 Ga Nuvvuagittuq (Porpoise Cove)  
866 greenstone belt, northeastern Superior Province, Canada. In: van Kranendonk, M. J.,  
867 Smithies, R. H., and Bennett, V. C. (eds) *Earth’s Oldest Rocks*. Elsevier, p.219-250.
- 868 PEARCE, J.A. 2003. Supra-subduction zone ophiolites: The search for modern analogues. In:  
869 DILEK, Y. & NEWCOMB, S. (eds) *Ophiolite Concept and the Evolution of Geological*  
870 *Thought*. Geological Society of America, Special Papers, **373**, 269-293.
- 871 POLAT, A. & HOFMANN, A.W. 2003. Alteration and geochemical patterns in the 3.7-3.8 Ga  
872 Isua greenstone belt, West Greenland. *Precambrian Research*, **126**, 197-218.
- 873 POLAT, A., HOFMANN, A.W. & ROSING, M.T. 2002. Boninite-like volcanic rocks in the  
874 3.7-3.8 Ga Isua greenstone belt, West Greenland: geochemical evidence for  
875 intra-oceanic subduction processes in the early Earth. *Chemical Geology*, **184**,  
876 231-254.
- 877 RIZO, H., BOYET, M., Blichert-Toft, J. & ROSING M. 2011. Combined Nd and Hf  
878 isotopic evidence for deep-seated source of Isua lavas. *Earth and Planetary Science*  
879 *Letters*, **312**, 267-279.
- 880 ROSING, M.T. 1999. <sup>13</sup>C-depleted carbon microparticles in >3700 Ma sea-floor sedimentary  
881 rocks from West Greenland. *Science*, **283**, 674–676.
- 882 ROSING, M.T, ROSE, N.M., BRIDGWATER, D. & THOMSEN, H.S. 1996. Earliest part of the  
883 Earth’s stratigraphic record: A reappraisal of the >3.7 Ga Isua (Greenland) supracrustal  
884 sequence. *Geology*, **24**, 43-46.
- 885 ROSING, M.T., BIRD, D.K, SLEEP, N.H. & BJERRUM, C.J. 2010. No climate paradox under  
886 the faint early Sun. *Nature*, **464**, 744-749.

- 887 SCHIDLOWSKI, M., APPEL, P.W.U., EICHMANN, R. & JUNGE, C.E. 1979. Carbon isotope  
888 geochemistry of the  $3.7 \times 10^9$ -yr old Isua sediments, West Greenland: implications for  
889 the Archaean carbon and oxygen cycles. *Geochimica et Cosmochimica Acta*, **43**,  
890 189-1899.
- 891 SCHIÖTTE, L., COMPSTON, W. & BRIDGWATER, D. 1989. Ion probe U-Th-Pb zircon dating  
892 of polymetamorphic orthogneisses from northern Labrador, Canada. *Canadian Journal*  
893 *of Earth Sciences*, **26**, 1533-1556.
- 894 SHERVAIS, J.W. 2001. Birth, death, and resurrection: The life cycle of suprasubduction zone  
895 ophiolites. *Geochemistry Geophysics Geosystems*, paper number 2000GC000080.
- 896 SHIREY, S.B. & RICHARDSON, S.H. 2011. Start of the Wilson cycle at 3 Ga shown by  
897 diamonds in the subcontinental mantle. *Science*, **333**, 434-436.
- 898 SOLVANG, M. 1999. An investigation of metavolcanic rocks from the eastern part of the Isua  
899 greenstone belt, Western Greenland. *Geological Survey of Denmark and Greenland*  
900 *(GEUS) Internal Report*, Copenhagen, Denmark, 62 pages.
- 901 STERN, R.J. & BLOOMER, S.H. 1992. Subduction zone infancy: examples from the Eocene  
902 Izu-Bonin-Mariana and Jurassic California arcs. *Geological Society of America*  
903 *Bulletin*, **104**, 1621-1636.
- 904 SUN, S.S. & MCDONOUGH, W.F. 1989. Chemical and isotopic systematics of oceanic  
905 basalts: Implications for mantle composition and processes. In: SAUNDERS, A.D. &  
906 NORRY, M.J. (eds) *Magmatism in the Ocean Basins*. Geological Society, London,  
907 Special Publications, **42**, 313-345.
- 908 VERVOORT, J.D., PLANK, T. & PRYTULAK, J. 2011. The Hf-Nd isotopic composition of  
909 marine sediments. *Geochimica et Cosmochimica Acta*, **75**, 5903-5926.
- 910

911 **Table captions**

912 Table 1. Summary of *c.* 3700 Ma crustal evolution in the Isua area, southern West Greenland.

913

914 Table 2. Whole rock geochemistry of *c.* 3700 Ma Isua rocks. See footnotes for analytical  
915 techniques and sources. Laser –ICP-MS trace element analyses were undertaken using fused  
916 discs.

917

918 **Figure captions**

919 Figure 1. Geological map of the Isua area, emphasising the *c.* 3700 Ma rocks and the tectonic  
920 contact with the *c.* 3800 Ma terrane to the south. Areas shown in Figures 2 and 4 are indicated.

921

922 Figure 2. Geological map of part of the northwestern Isua supracrustal belt. U-Pb zircon age  
923 constraints (Nutman & Friend, 2009 and Friend & Nutman, 2010 and references therein) are  
924 given with 95% confidence uncertainties.

925

926 Figure 3. (A) Dunite from the large mantle-derived ultramafic pod in the northeastern part of  
927 Fig. 2 (pen for scale, bottom right). Fine-grained olivine matrix contains larger orientated  
928 olivine grains (running left-right in the photograph). This fabric formed at high temperature in  
929 the mantle, not in the crust during amphibolite facies metamorphism (Friend & Nutman, 2011).  
930 (B) Back scattered electron image of dunite. Grey = forsteritic olivine; black = secondary  
931 serpentine and white = secondary magnetite. The small amount of secondary magnetite reflects  
932 the very high Mg/Fe ratio of the rock. Note the polygonal texture.

933

934 Figure 4. Geological map of part of the eastern Isua supracrustal belt. U-Pb zircon age  
935 constraints (Nutman & Friend, 2009 and Friend & Nutman, 2010 and references therein) are  
936 given with 95% confidence uncertainties.

937

938 Figure 5. Isua *c.* 3700 Ma rocks in the mafic igneous (M) – felsic igneous (F) – weathering (W)  
939 plot of Ohata & Arai (2008). See Ohata & Arai (2008) for how these parameters are



940 constructed. This plot is applicable for all igneous compositions from basalts to granites. This  
941 plot includes data from a figure in Nutman *et al.* (2012a).

942

943 Figure 6. Geochemistry plots of Isua *c.* 3700 Ma mafic and intermediate igneous rocks. (A)  
944 Primitive mantle normalised trace element diagrams (normalised with values of Sun &  
945 McDonough, 1989), (B) Nb/Yb versus Th/Yb, with fields from Pearce (2003).

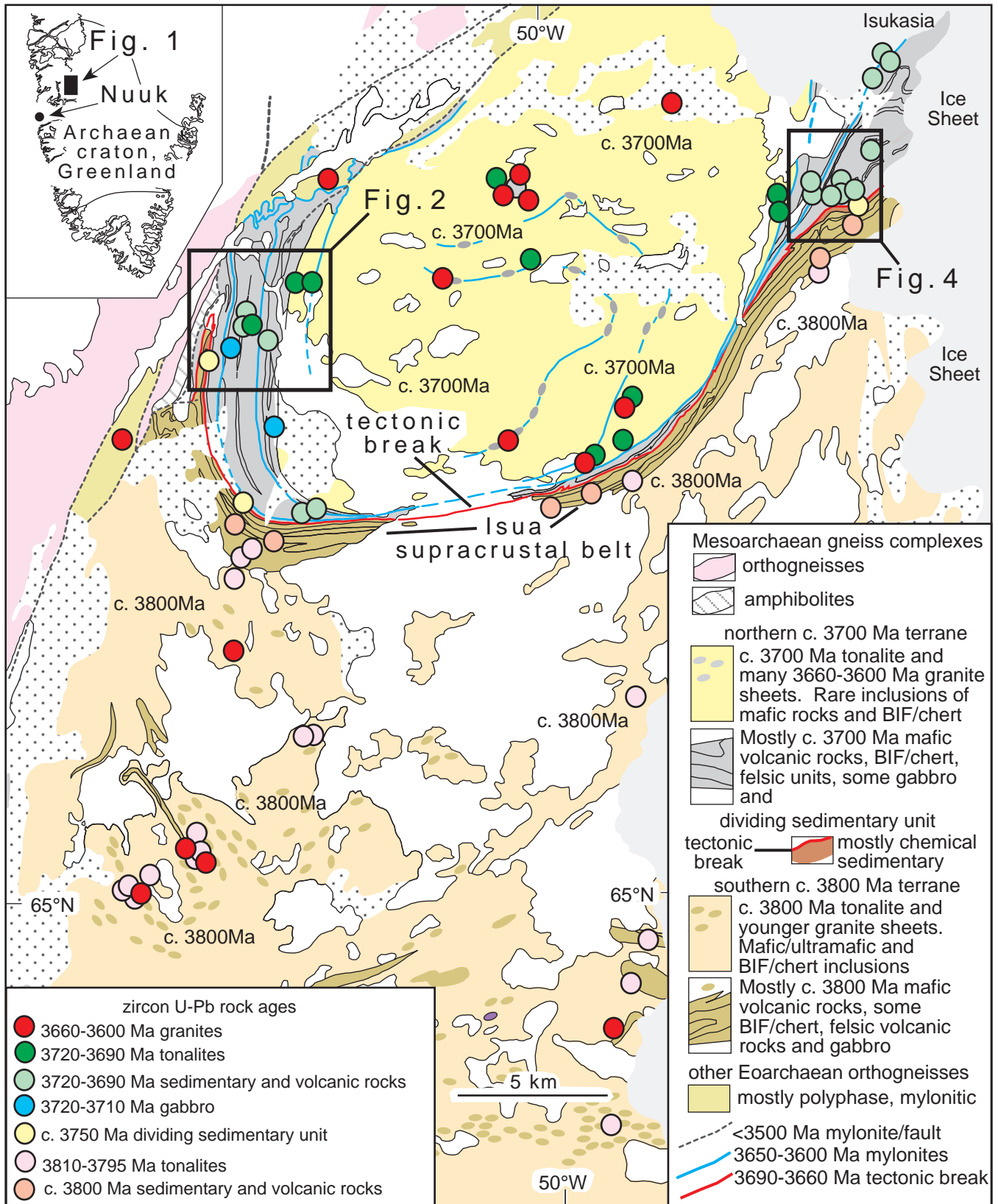
946

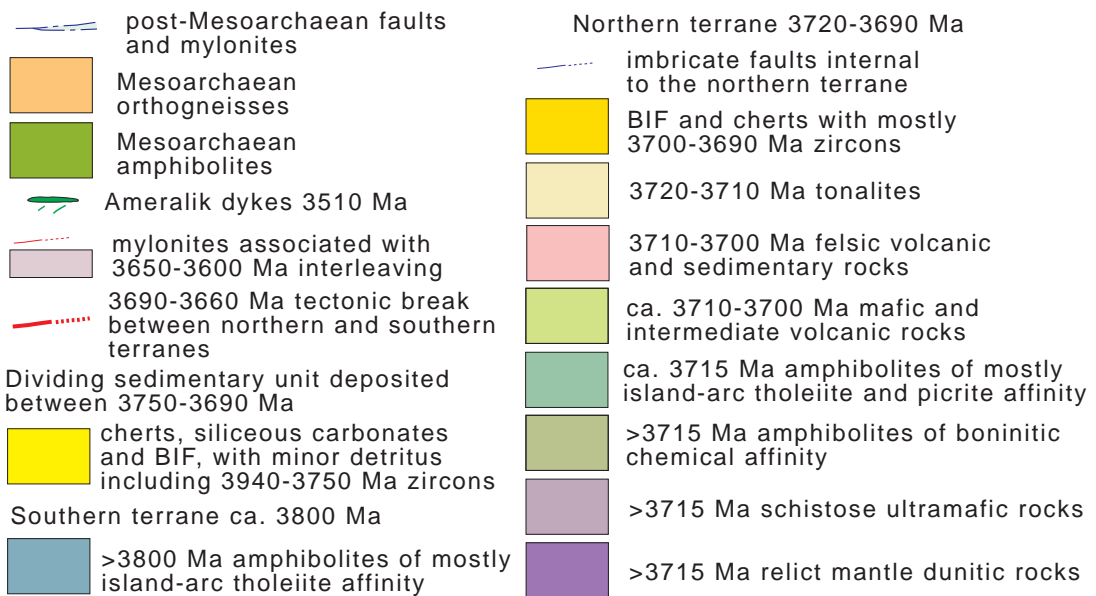
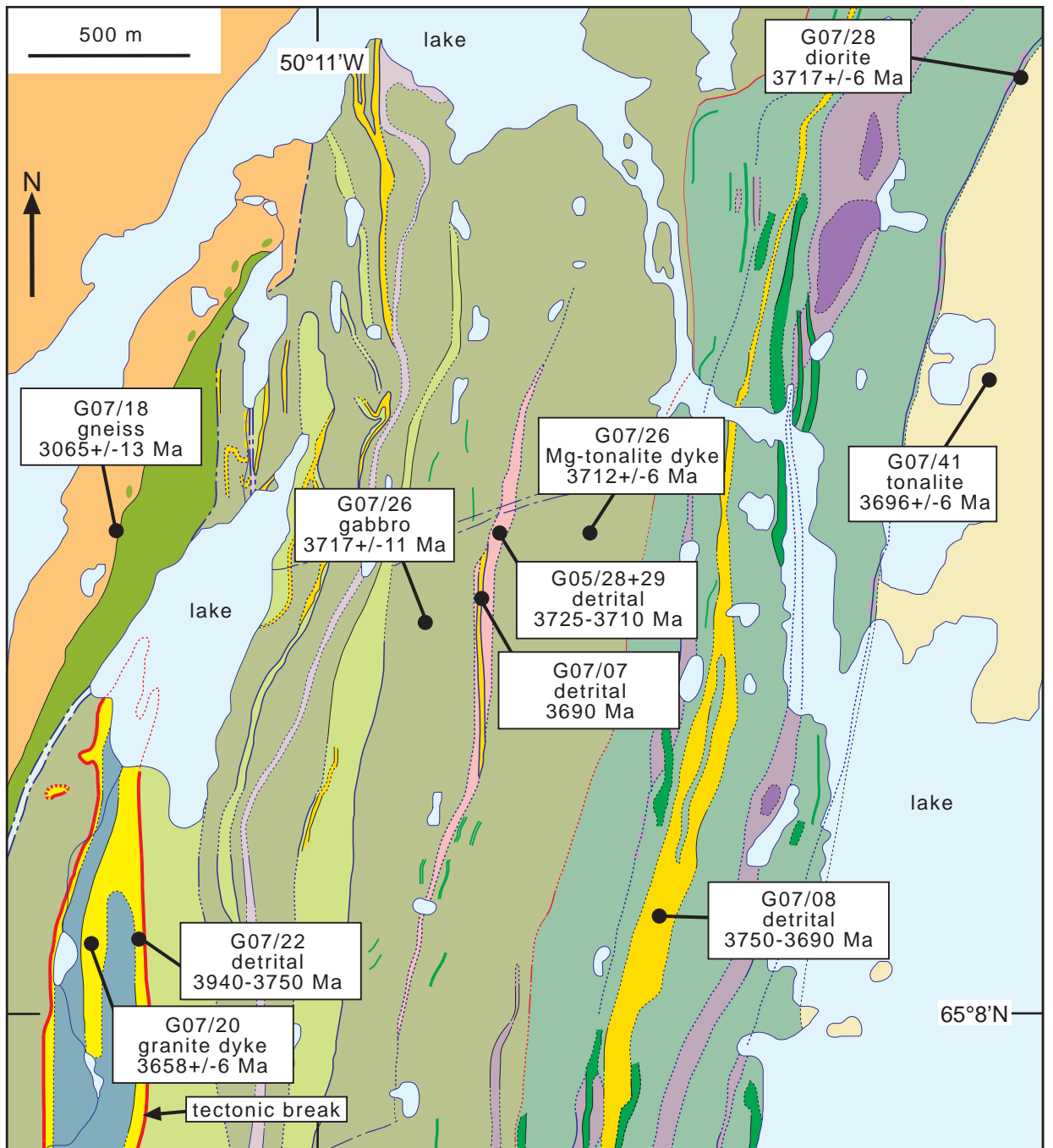
947 Figure 7. Geochemistry of *c.* 3700 Ma felsic igneous rocks: (A) SiO<sub>2</sub> versus MgO, (B) Y versus  
948 Sr/Y and (C) Yb<sub>(N)</sub> versus La/Yb<sub>(N)</sub>/Yb<sub>(N)</sub>. TTG = tonalite-trondhjemite-granodiorite. The  
949 fields in the trace element diagrams are taken from Martin (1986). Rare earth elements are  
950 normalised to chondrite, using the values of Sun & McDonough (1989).

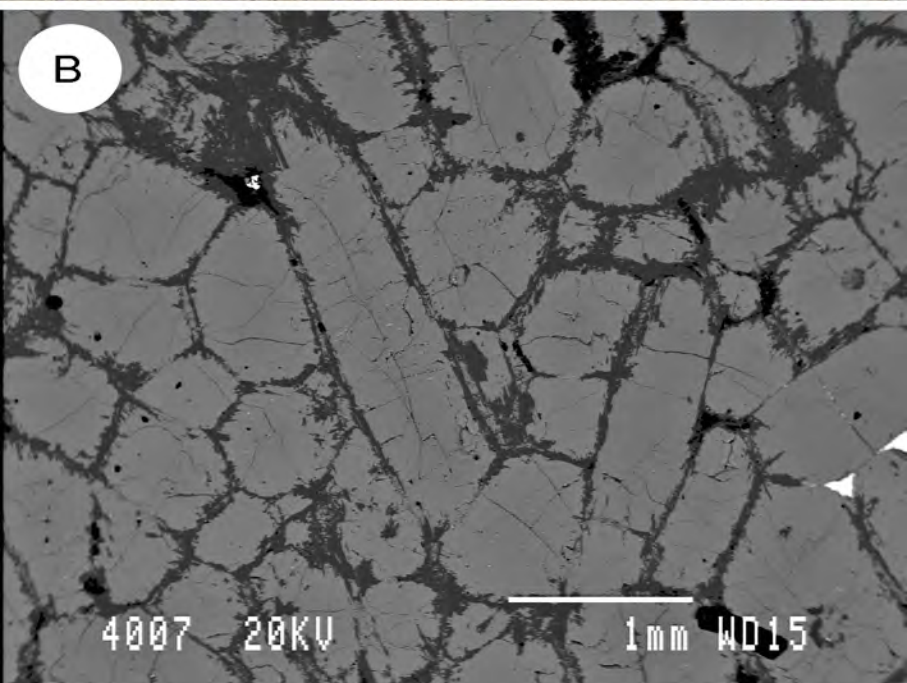
951

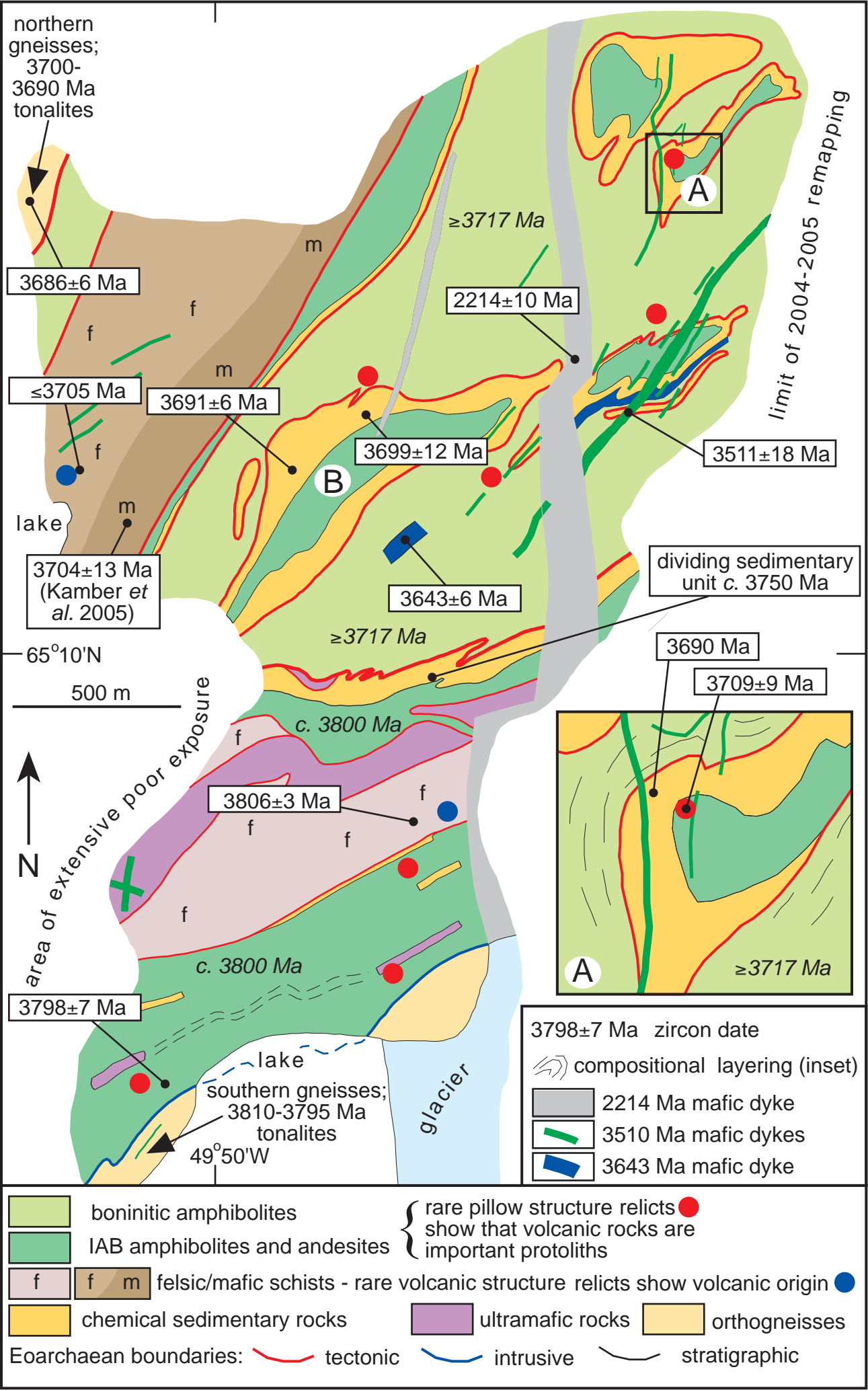
952 Figure 8. Cartoon cross sections comparing *mature* Eoarchaeon proto-arc and Phanerozoic  
953 island arc structure. The proto-arc is shown at the dominant tonalite-dacite producing phase,  
954 *after* arc initiation when fluid fluxing of a mantle wedge occurred.

955

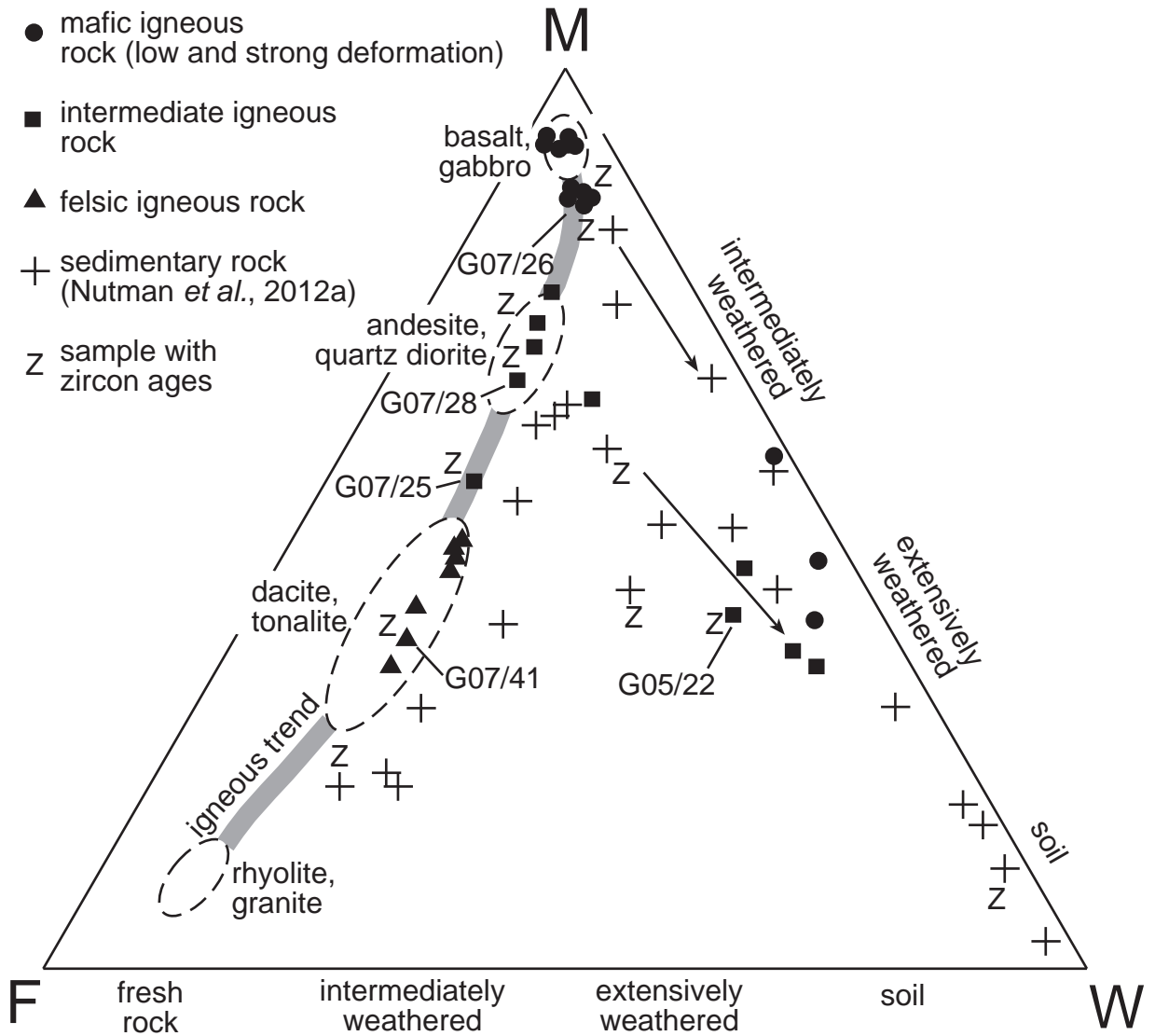


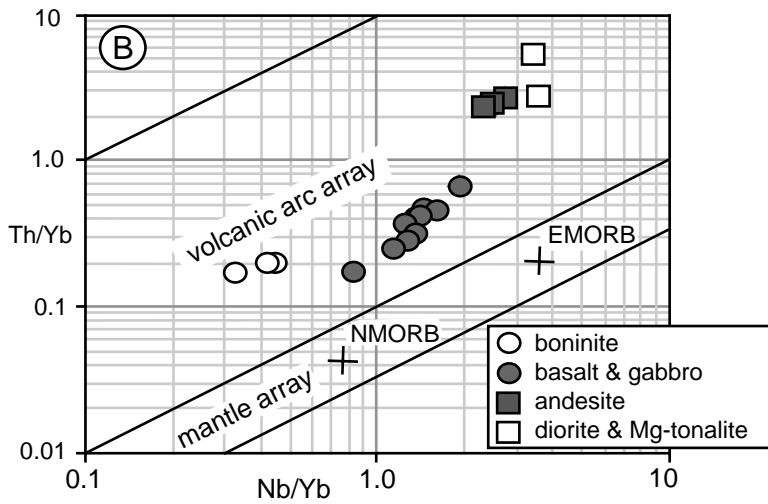
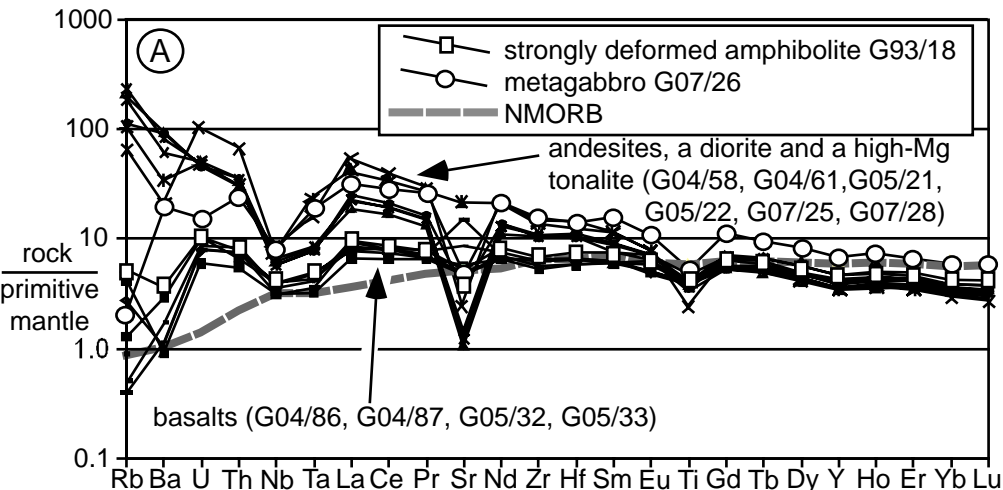


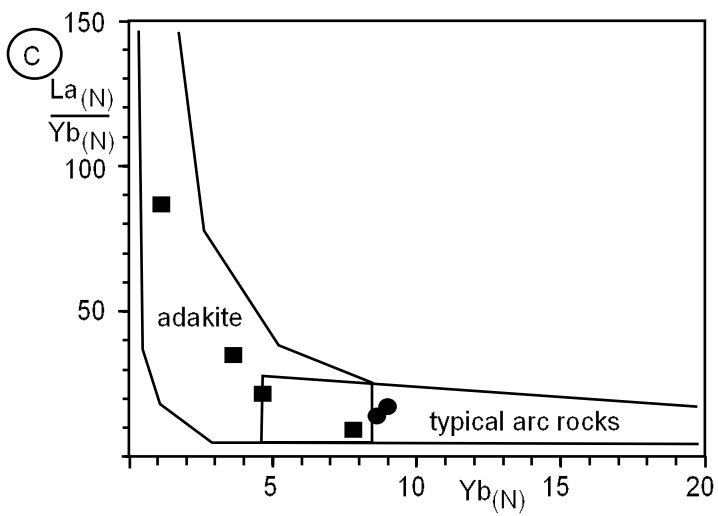
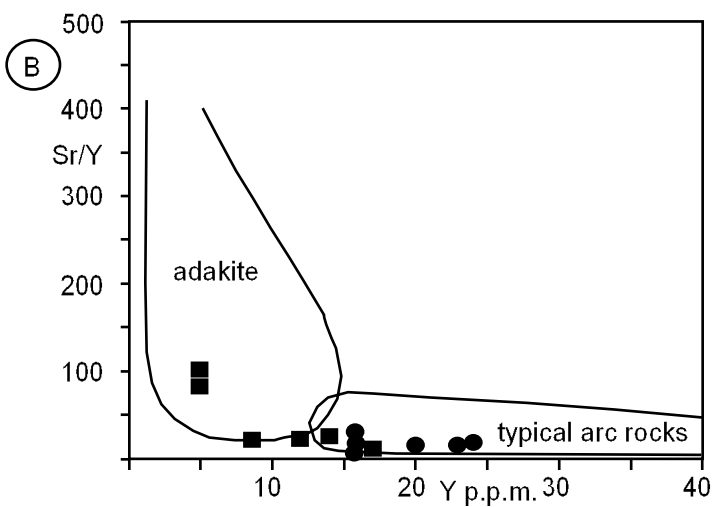
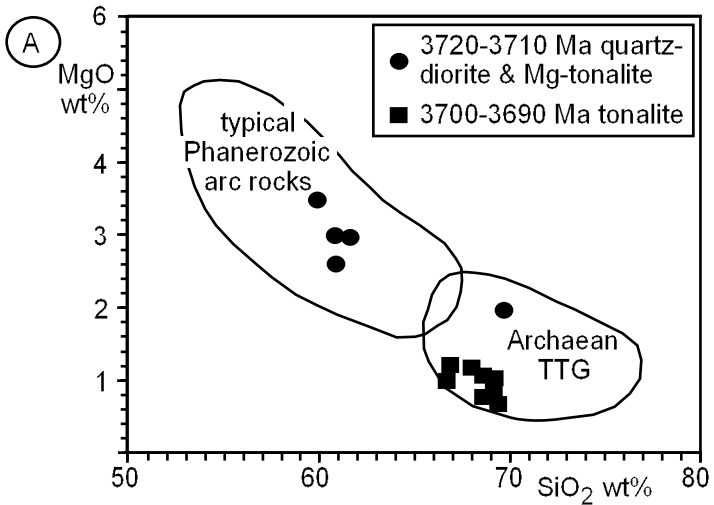






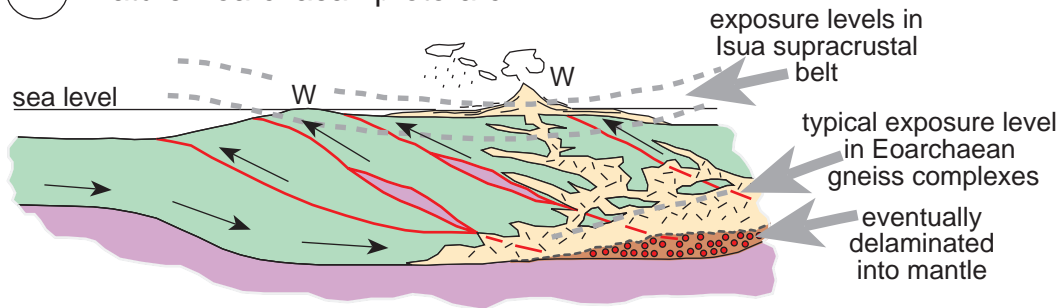




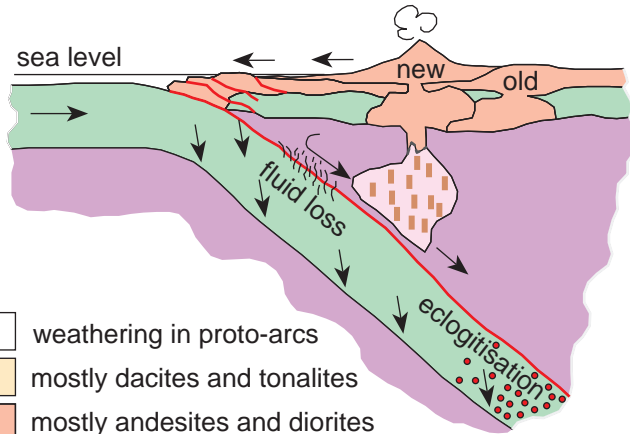




(A) Mature Eoarchaean proto-arc



(B) Mature Phanerozoic island arc



- W weathering in proto-arcs
- mostly dacites and tonalites
- mostly andesites and diorites
- non-discriminated basaltic crust
- melting of eclogitised basaltic crust
- melting of metasomatised mantle
- basaltic crust eclogitised after fluid loss
- mantle
- ← ↓ motion of lithosphere